5-2005

The Inverse Application of Conformal Mapping Techniques to Describe Groundwater Flow-Regimes through a Window in the Upper Claiborne Confining Layer

Patrick Lasater McMahon
University of Tennessee, Knoxville

To the Graduate Council:

I am submitting herewith a thesis written by Patrick Lasater McMahon entitled "The Inverse Application of Conformal Mapping Techniques to Describe Groundwater Flow-Regimes through a Window in the Upper Claiborne Confining Layer." I have examined the final electronic copy of this thesis for form and content and recommend that it be accepted in partial fulfillment of the requirements for the degree of Master of Science, with a major in Environmental Engineering.

Randall Gentry, Major Professor

We have read this thesis and recommend its acceptance:

John Schwartz, Larry McKay

Accepted for the Council:
Carolyn R. Hodges

Vice Provost and Dean of the Graduate School

(Original signatures are on file with official student records.)

To the Graduate Council:

I am submitting herewith a thesis written by Patrick Lasater McMahon entitled "The Inverse Application of Conformal Mapping Techniques to Describe Groundwater Flow-Regimes through a Window in the Upper Claiborne Confining Layer." I have examined the final paper copy of this thesis for form and content and recommend that it be accepted in partial fulfillment of he requirements for the degree of Master of Science, with a major in Environmental Engineering.

Randall Gentry, Major Professor

We have read this thesis
and recommend its acceptance:

John Schwartz

Larry McKay

Accepted for the Council:

Vice Chancellor and
Dean of Graduate Studies

The Inverse Application of Conformal Mapping Techniques to Describe Groundwater Flow-Regimes through a Window in the Upper Claiborne Confining Layer

A Thesis
Presented for the
Master of Science
Degree
The University of Tennessee, Knoxville

Patrick Lasater McMahon
May 2005

Acknowledgments

I would like to thank my major professor, Dr. Randall Gentry, for his assistance in the development of the research and for his tireless positive nature. I would like to thank Dr. Erik Anderson for his personal correspondence and guidance in the application of his analytic element modeling equations. I would also like to thank the other members of my committee Dr. John Schwartz and Dr. Larry McKay for their time and expertise in developing this paper. Finally I would like to thank my family and friends for all their encouragement and understanding.

Abstract

The purpose of this study was to establish an inverse algorithm to solve the analytic element groundwater modeling equations, developed by Anderson (2001), for state parameters based on head data from an appropriate field site. The analytical element model (AEM) equations developed by Anderson (2001) are a complex variable technique to describe flow regimes through a gap in a confining layer that otherwise separates two confined aquifers. Anderson's equations are based on the assumptions that hydraulic conductivity is constant in the respective confined aquifers. It also assumes a hydraulic conductivity of zero for the confining layers in the system.

A Levenberg-Marquardt based inverse algorithm was developed and applied to synthetic data created by the forward application of Anderson's AEM equations based on state variables similar to those presented in the literature (Anderson 2001). The inverse algorithm was used to solve for the state parameters describing *window length* (L) and *flux through the window* (Q) given four head values observed in the forward solution. The inverse algorithm successfully predicted values for window length and flux through the window within 20% of the values used to create the synthetic head data. A study on the effect of an added observation point in the flow field was also performed. It was observed that an added observation point in the flow field resulted in better approximations of L and Q by the inverse algorithm.

The algorithm was then applied to an actual field case, the Shelby Farms Site in Memphis, Tennessee, in an attempt to predict the window extent and flux through the window based on head observations from four wells installed within the window. Based on data from three separate occasions, the algorithm produced a value for window length of L= 573.9 ft and flow through a unit slice of the window of Q= -525.0 ft^3/day, which compares well with the value of 35,627 ft^3/day for the entire window profile from other recent studies at the Shelby Farms Site.

Table of Contents

Table of Contents (Continued)

List of Tables

List of Figures

1 Introduction

1.1 Groundwater Management

Proper Management of a groundwater system requires an understanding of both the hydraulic characteristics of the system and how meaningful observations may be made to ascertain the state of the system. The use of groundwater modeling techniques is a common means to achieve this understanding. The application of forward modeling techniques is useful to better understand the reaction of these systems to given changes. Thus, aiding in the a overall understanding of the hydraulic characteristics associated with a particular site. An understanding of how meaningful observations may be made in order to ascertain the state of a given system can be achieved by the exploration and application of inverse modeling techniques. When coupled with a forward modeling technique the usefulness of observation data, such as head values, in defining the state of a system can be maximized.

One particular type of system where the relationship between observations and system states is not fully understood is a focused recharge system. Areas of focused recharge include sites where two systems that would otherwise be separated are connected over a relatively small area, known as a window. Understanding the flow paths at these sites becomes important when one system is potentially compromising the water quality of the other. Recently the Committee on Hydrologic Science, of the National Research Council, addressed the basic scientific questions regarding diffuse versus focused recharge in hydrogeologic settings (NRC 2004). They concluded that methodologies for better predicting system flow paths based upon state observations are needed for a more thorough understanding of focused recharge system behaviors.

1.2 Inverse Modeling

Sun (1995) observes that the study of forward modeling problems has advanced rapidly since the advent of computers. Complicated systems such as three-dimensional multicomponent transport in multiphase flow can be simulated with relative ease (Sun 1995). However, the study of inverse modeling has not progressed as rapidly. Presently, the study of inverse problems in groundwater modeling is limited to the consideration of very simple models (Sun 1995). A comprehensive survey of inverse procedures is provided in the literature by Yeh (1986), who is considered one of the pioneering researchers in the area of inverse modeling theory. Yeh presents the theory that inverse modeling can be approached by formulating the model into a traditional optimization problem. The inverse problem is defined in terms of a goal to minimize an error function that represents the difference between a known state of the system compared to a simulated state.

Often this state is defined in terms of system heads. Inverse modeling provides an opportunity to directly estimate system parameters that dictate head distributions and flow paths given head data collected in the field. In the case of a focused recharge site, a recently developed forward model, Anderson (2001), in conjunction with an inverse modeling technique could be used to estimate unknown system parameters such as flux through the window given local head measurements.

1.3 Research Hypothesis and Objectives

The goal of this research was to apply an inverse modeling technique for the purpose of better understanding flow paths in and near aquitard windows as focused recharge features. The research hypothesis was that the analytical element model

developed by Anderson (2001) could be solved inversely for the parameters *window length* and *flux through the window* based upon head observations in and near a window feature. Furthermore, that this inverse modeling algorithm can provide a uniform flow field estimation from actual field data. Testing of the research hypothesis required the completion of the following objectives:

1. Development of synthetic datasets based on data provided in the literature by Anderson (2001);

2. Development of an inverse algorithm using the Levenberg-Marquardt optimization technique coupled to Anderson's (2001) analytic element model;

3. Experimentally test the capability of the inverse algorithm to identify a solution using the synthetic data as the observation source; and

4. Use the inverse algorithm to develop a flow field realization based upon field data collected from the Shelby Farms window site in Memphis, Tennessee.

2 Background Information

2.1 Analytic Modeling

The use of analytically derived mathematical equations to approximate steady flow paths in porous media is a technique known as analytical modeling. To apply this technique, actual groundwater flow problems must be approximated into simpler ones that can be solved analytically yet, still provide insight into the essence of the real problem (Strack 1989). In cases where the problem cannot be handled adequately by simple means and recourse to a numerical solution is necessary, the determination and interpretation of relatively crude approximate solutions often provides insight that can be used in selecting and setting up the numerical model that will ultimately be used to solve the problem (Strack 1989).

Analytical equations describing flow in porous media are based on Darcy's Law (Darcy 1856). When Darcy's Law is combined with the continuity equation, a governing relationship for steady flow of a homogeneous fluid in a porous medium results. Many analytic solutions describing flow have been developed based on this relationship (Strack 1989, Polubarinova-Kochina 1962, Heitzman 1977, Sidiropoulos et al. 1983). The act of superimposing one analytic solution onto another in an effort to describe a more elaborate system is known as the *analytic element method.* Models resulting from this procedure are known as *analytic element models* (AEM).

2.2 Conformal Mapping as an Analytical Technique

Conformal mapping is a complex variable technique that has been used extensively in the field of groundwater mechanics (Strack 1989). This technique involves the use of a conformal transformation that maps complex variables from the

physical plane into an intermediate plane where the calculation of the equations governing flow in the system are performed. The same conformal transformation is then used to map the solution back into the physical plane were the resulting flow field can be observed. Conformal mapping equations are used in groundwater mechanics to simplify boundary value problems that would otherwise be solved with the application of the Laplace equation.

In the field of water resources, conformal mapping has been used to describe flow in situations such as flow under dams, around bridge pilings, and between aquifers and streams. One of the benefits to using conformal mapping is that a two-dimensional closed form solution can be obtained with the input of relatively few parameters. Deterministic modeling packages such as MODFLOW can produce three-dimensional assessments of groundwater flow fields but require a large number of data points. Before computers were in common use, closed form solutions were the best way to obtain quantitative answers to groundwater flow problems. Many of these conformal mapping closed form solutions were published in the mid to late 1900s (Obdan ANM and Veling EJM, 1987, Kacimov AR, Obnosov 2000). Conformal mapping is still a very useful tool to obtain solutions to simplified versions of complex problems (Strack, 1989).

2.3 Development of Anderson's Analytic Element Modeling Equations

The analytical element model developed by Anderson (2001) is built on classical solutions based on the method of images for circular boundaries. The transformation is shown below.

$$z = -\left(\frac{L}{4}\right) * \left(\zeta + \frac{1}{\zeta}\right)$$

z= complex value in the z plane
L= one-dimensional window length
ζ= complex value in the ζ plane

This transformation maps concentric circles centered on the origin of the ζ plane onto confocal ellipses with foci at x=±L/2 in the z plane, ***Figure 2.1*** (Anderson, 2001).

Flow field solutions are obtained by contouring the real and imaginary components of the complex potential in the z plane. The complex potential is defined as:

$$\Omega = \Phi + i\Psi$$

$$\Phi = kb\varphi$$

k= hydraulic conductivity
b= aquifer thickness normal to the z plane
φ= hydraulic head
Ψ= stream function

The complex potential is defined in the ζ plane, and for the given geometry is calculated with the application of the following boundary condition for uniform flow in theζ plane (Strack 1989):

$$\Omega = \left(\frac{1}{4}\right) Q_{xo} L\zeta + \Phi_0$$

Ω= the complex potential
Q_{x0}= flow along the real axis
ζ= complex value in the ζ plane
L= one-dimensional window length
Φ_0= value of the potential along the imaginary axis of the z plane

Combining this equation with the given transformation and rewriting the resulting equation in terms of Ω results in the following in which Ω is calculated in the z plane:

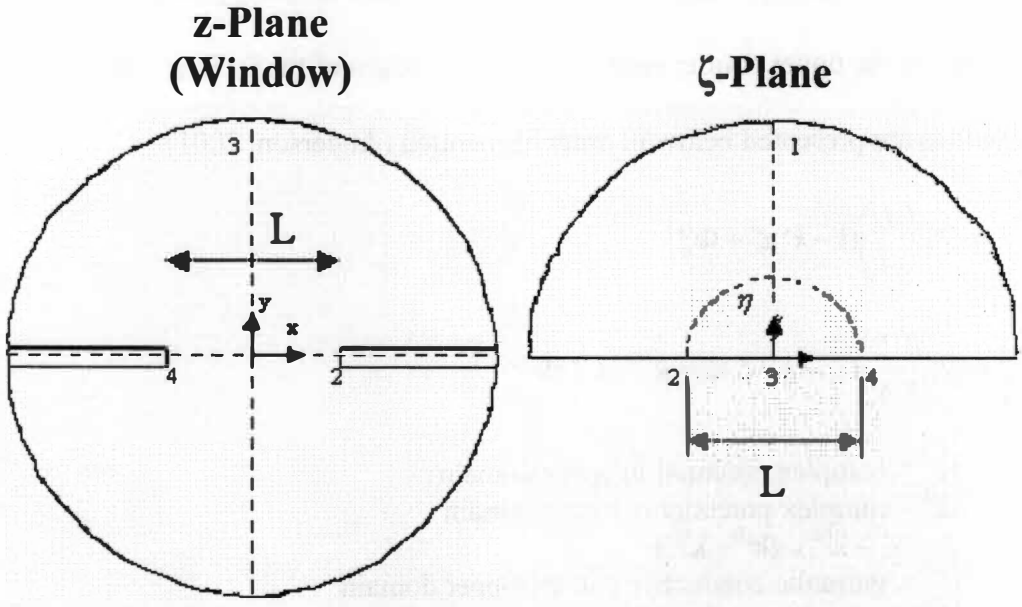

Adapted from Anderson (2001)

Figure 2.1 Visual Representation of the z and ζ Planes.
The z plane represents the physical plane of the problem and the ζ plane exists as an intermediate plane in which calculations are carried out. Answers calculated in the ζ plane are conformaly mapped on the z plane to obtain a flow field realization. The numbers and dashed lines indicate lines and points of symmetry.

$$\Omega = -\frac{1}{2}Q_{x0}\left[z \pm \sqrt{\left(z-\frac{L}{2}\right)\left(z+\frac{L}{2}\right)}\right] + \Phi_0$$

Anderson's calculation of the complex potential is the superposition of the classical solutions of uniform flow past a circular inhomogeneity with flow along the x-axis, flow at infinity in the upper aquifer with uniform no-flow at infinity in the lower aquifer, and flow to the upper aquifer with a drain at the origin of the ζ plane. These classical solutions are presented below in order of mention (Anderson, 2001).

1. $$\Omega^{(u)} = Q_{x0}^{(l)}\left(\frac{L}{4}\right)(1-k')\zeta + \Phi_0^{(u)}$$

$$\Omega^{(L)} = Q_{x0}^{(l)}\left(\frac{L}{4}\right)(\zeta - k'/\zeta)\zeta + k^{(l)}/k^{(u)}\Phi_0^{(u)}$$

$\Omega^{(u)}$= complex potential in upper domain
$\Omega^{(l)}$= complex potential in lower domain
$k' = (k^{(l)} - k^{(u)})/(k^{(l)} + k^{(u)})$
$k^{(u)}$= hydraulic conductivity in the upper domain
$k^{(l)}$= hydraulic conductivity in the lower domain

2. $$\Omega^{(u)} = Q_{x0}^{(u)}\left(\frac{L}{4}\right)\left(\frac{1}{\zeta} - k'\zeta\right)$$

$$\Omega^{(u)} = Q_{x0}^{(u)}\left(\frac{L}{4}\right)(1+k')\left(\frac{1}{\zeta}\right)$$

3. $$\Omega^{(u)} = \left(\frac{Q}{\pi}\right)\ln\zeta$$

$$\Omega^{(l)} = \left(\frac{Q}{\pi}\right)\ln\zeta$$

The superposition of these solutions forms the following equation set:

$$\Omega^{(u)} = \left[Q_{x0}^{(l)}(1+k') - Q_{x0}^{(u)}k'\right]\left[\frac{L}{4}\right)\zeta + Q_{xo}^{(u)}\left(\frac{L}{\zeta 4}\right) + \left(\frac{Q}{\pi}\right)\ln\zeta + \Phi_0^{(u)}$$

$$\Omega^{(l)} = Q_{x0}^{(l)}\left(\frac{L}{4}\right)\zeta + \left[Q_{x0}^{(u)}k' + Q_{xo}^{(u)}(1+k')\right]\left(\frac{L}{4\zeta}\right) + \left(\frac{Q}{\pi}\right)\ln\zeta + \left(\frac{k^{(l)}}{k^{(u)}}\right)\Phi_0^{(u)}$$

$\Phi_0^{(u)}$= constant evaluated from a reference point on the imaginary axis of the z plane with known head

This equation set constitutes the analytic element model that Anderson (2001) developed to describe flow through a window between two aquifers of differing hydraulic conductivity. These equations are used in conjunction with the mapping transformation given at the start of the discussion to produce a map of the flow field in the z-plane.

The complex potentials are solved for based on their location in the z-plane. Initial value of a point in the z-plane is equal to the complex coordinate of that point. After the application of Anderson's AEM the value of the same point in the z-plane is the complex value corresponding to the head at that point (the real value) and the stream tube value (the imaginary value). By contouring these grids of values the flow field can be observed.

2.4 Gauss-Newton Optimization

In order to develop an inverse algorithm with Anderson's AEM, an optimization technique was applied. The Gauss-Newton method is a traditional non-linear optimization technique. It is applied as an inverse technique by defining an objective

function of the sum of the squares of error in predicted heads verses the heads in the known flow field. The goal of the optimization is to minimize this objective function.

$$E(k) = \sum_{l=1}^{L} w^2 \left[u(k) - u_{obs}\right]^2$$

E(k)= sum of the squares of error
w= weighting value
u(k)= forward model output
u_{obs}= field data

For clarity we will write $w^2\left[u(k) - u_{obs}\right]^2$ simply as f (k). The theory behind the application is based upon defining a search area near the global optimal value. The technique will mathematically determine the local minima by the determination of a positive-definite Hessian matrix. The procedure begins with taking the second order partial derivative of E(k), the second order terms on the right-hand side of the resulting equation are assumed to be negligible (Sun 1995).

Thus,

$$\frac{\partial^2 E}{\partial k_i \partial k_j} \approx 2\sum_{l=1}^{L} \frac{\partial f_1}{\partial k_i} \frac{\partial f_1}{\partial k_i}.$$

The following matrix is defined, which consists of derivatives of functions f_1(k), f_2(k),… f_m(k) with respect to the variation of each parameter component k_1, k_2, …k_n.

$$A = \begin{bmatrix} \frac{\partial f_1}{\partial k_1} & \frac{\partial f_2}{\partial k_2} & \cdots & \frac{\partial f_1}{\partial k_n} \\ \frac{\partial f_2}{\partial k_1} & \frac{\partial f_2}{\partial k_2} & \cdots & \frac{\partial f_2}{\partial k_n} \\ \vdots & \vdots & \ddots & \vdots \\ \frac{\partial f_m}{\partial k_1} & \frac{\partial f_m}{\partial k_2} & \cdots & \frac{\partial f_m}{\partial k_n} \end{bmatrix}$$

The matrix is typically not square due to the fact that in an inverse modeling problem the number of observations f (k) outnumbers the number of parameters for identification yielding added degrees of freedom. With the use of matrix [A] and the application of the equations for first and second order partial derivatives given above, the gradient can be represented by

$$\nabla E = 2A^T f$$

where;

$$f = (f_1, f_2, \ldots, f_L)^T .$$

The Hessian matrix G can be approximately represented by

$$G \approx 2A^T A .$$

Substituting the equation for the gradient and the approximation of the Hessian matrix into Newton algorithm the following equation is derived.

$$k_{n+1} = k_n - (A_n^T A_n)^{-1} A_n^T f_n$$

The iteration sequence generated by this equation is the Gauss-Newton sequence (Sun 1995).

$$\Delta k_n = -(A_n^T A_n)^{-1} A_n^T f_n$$

The Gauss-Newton direction is determined solely by the first order derivatives. It is pertinent to mention that when $f_1, f_2, \ldots, f_L$ are nonlinear functions, the deviation of the Gauss-Newton direction depends on the error in the assumption that $G \approx 2A^T A$. For small residual problems the Gauss-Newton sequence converges rapidly. However, in groundwater modeling, parameter identification problems produce residuals that are often very large. This condition leads to the following difficulties (Sun, 1995):

1. The search sequence will not converge because for some n $E(k_{n+1}) > E(k_n)$.

2. The Gauss-Newton direction cannot be determined because the matrix $A^T A$ is nearly singular.

3. The value Δk_n is so large that k_{n+1} is outside of the range of admissible values.

2.5 Modified Gauss-Newton Optimization

There are many ways to modify the Gauss-Newton algorithm to overcome the problems mentioned in section 2.4. One of these modifications involves the addition, to the values of $A_n^T A_n$, of a uniform factor, λ. The equation for Δk_n then becomes:

$$\Delta k_n = -(A_n^T A_n + I\lambda)^{-1} A_n^T f_n$$

I= identity matrix

$\lambda = 10\text{^}x$

The factor of x by which ten is raised can vary widely. Its exact value is determined each time an iteration is run in order to satisfy $E(k_{n+1}) > E(k_n)$. This modification relieves problems 1 and 2 mentioned in section 2.4. This modified form of the Gauss-Newton optimization is known as the Levenberg-Marqardt optimization and is the optimization method of choice to attempt to inversely apply Anderson's AEM.

3 Methods

3.1 Development of Synthetic Datasets Based on the Analytical Element Model Developed by Anderson (2001)

In order to develop and evaluate the inverse algorithm, synthetic datasets were first created. With these synthetic datasets, head values were collected from the forward modeling of known values of *window length* and *flux through the window*. Thus, the inverse algorithm developed was evaluated by its ability to start at an initial guess for these parameters and arrive at a solution close to the known values.

3.1.1 Forward Modeling of the First Synthetic Test Case

The parameters used in the literature by Anderson (2001) to illustrate the AEM were used to develop the first synthetic test case. Though Anderson (2001) makes no mention of units in his flow field figure, it was assumed that the figure is a unit block with data points calculated on a scale fine enough to give a clear resolution of the contoured values. For the calculation of the complex potential, a square unit grid with complex potentials calculated on 1/1000-unit increments was used. For clarity we will consider the grid to be 200 ft by 200 ft. Thus, values are calculated in 0.2 ft increments for a total of one million calculations of the complex potential in a single grid.

Parameter values were chosen to be consistent with the ratios presented by Anderson (2001).

$$\frac{Q}{Q_{x0}^{(l)}L} = \frac{1}{3}$$

$$\frac{k^{(u)}}{k^{(l)}} = 3$$

$$\frac{Q_{x0}^{(u)}}{Q_{x0}^{(l)}} = -\frac{1}{3}$$

The window length was chosen to be .5 units, or 100 feet, and the flow through the window was chosen to be 100 ft^3/day to meet Anderson's ratio requirements. Thus the parameter values used in the first synthetic case were:

$$L = 100\,ft \qquad k^{(u)} = 3\frac{ft}{day}$$

$$Q = 100\frac{ft^3}{day} \qquad k^{(l)} = 1\frac{ft}{day}$$

$$Q_{x0}^{(u)} = -1\frac{ft^3}{day} \qquad \phi = 1\,ft$$

$$Q_{x0}^{(l)} = 3\frac{ft^3}{day} \qquad b = 1\,ft$$

An Excel spreadsheet was first used to calculate the one million complex potentials for the synthetic data point collection. However, this approach was abandoned due to problems associated with data management. A FORTRAN program, which proved much more efficient, was written to carry out the calculations (Appendix A).

The FORTRAN program creates three output files based on the input file `conformal.in`, which contains values for the eight input parameters. The file `con_head.out` is an ASCII grid file containing one million head values calculated on the 0.2 ft interval. The file `con_stream.out` is an ASCII grid file containing one million stream tube values calculated on the 0.2 ft interval. The third output file is `well_head.out`. This file only reports four values. These values are the head values for

the four head observation points shown in ***Figure 3.1***. These points represent synthetic well screens and were chosen with a vertical placement similar to observation wells that might be located within a window (i.e. such as the Shelby Farms window site in Memphis, Tennessee); see ***Figure 3.2***. These values were recorded as the "field" head measurements to be used as the state variables in the inverse algorithm. The ASCII files representing stream and head values were both imported into ArcView GIS and contoured, see ***Figure 3.1***. Head values reported by the output file `well_heads.out` were recorded as the "field" head values for synthetic dataset one

3.1.2 Forward Modeling of the Second Synthetic Test Case

A second synthetic dataset was chosen so that the values of parameters describing *window length* and *flow through the window* were different in value and magnitude from the first test case. This was done to assure that the successful application of the inverse algorithm was robust with respect to the parameters L and Q. Thus the values of L and Q chosen for use in the second synthetic test case are shown below.

$$L = 173\,ft \qquad k^{(u)} = 3\frac{ft}{day}$$

$$Q_{x0}^{(u)} = -1\frac{ft^3}{day} \qquad k^{(l)} = 1\frac{ft}{day}$$

$$Q_{x0}^{(l)} = 3\frac{ft^3}{day} \qquad \phi = 1\,ft$$

$$Q = 113\frac{ft^3}{day} \qquad b = 1\,ft$$

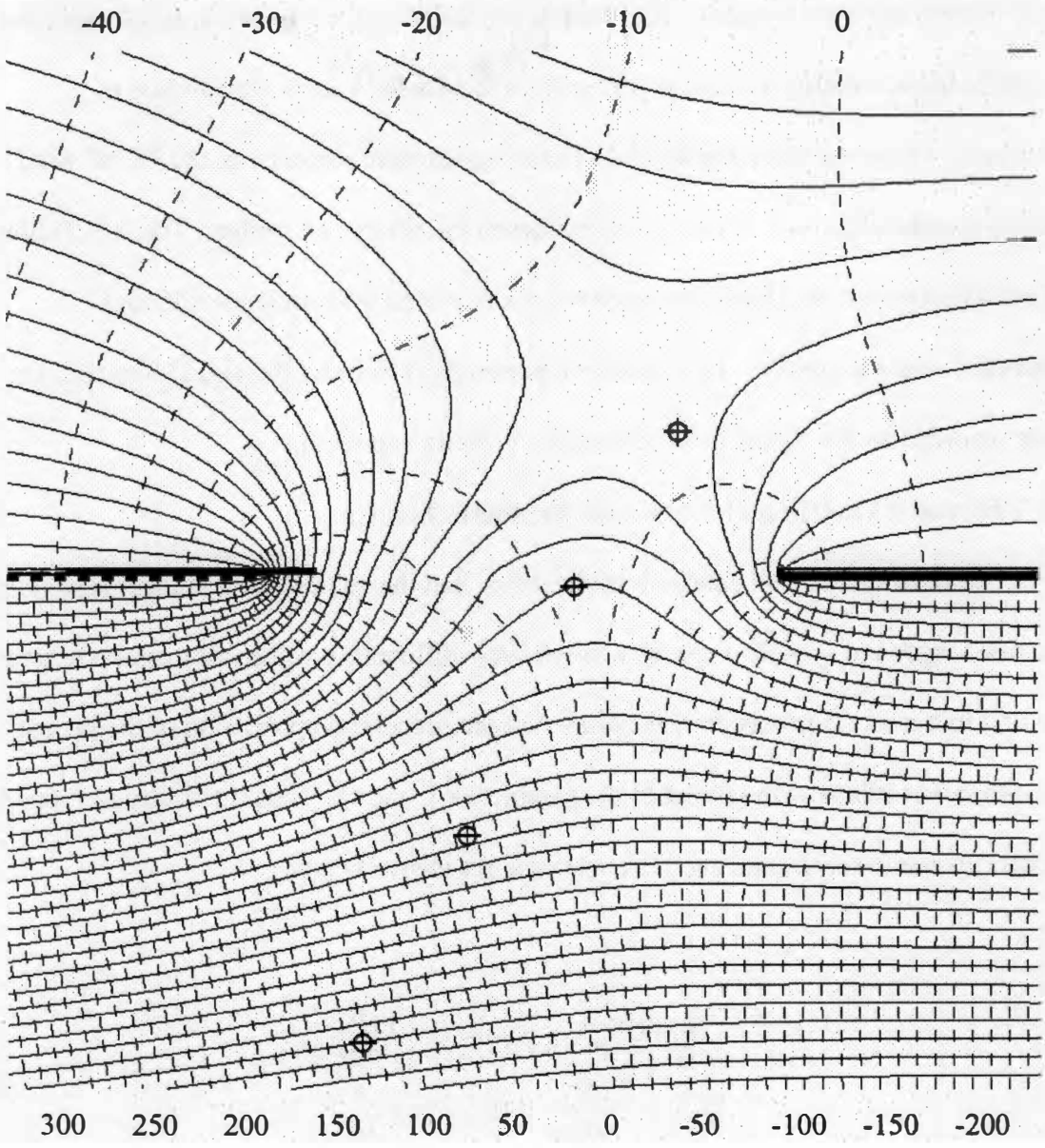

Figure 3.1 Synthetic Dataset One Based Upon Anderson (2001).
This figure represents a vertical cross section through a window of unit width normal to the vertical plane. All head values are presented in feet.

L=100 ft Q=100ft^3/day

---------- Head Contours

_____ Flow Paths

100 ft

Scale

⊕ Location of Synthetic Data Point Collection

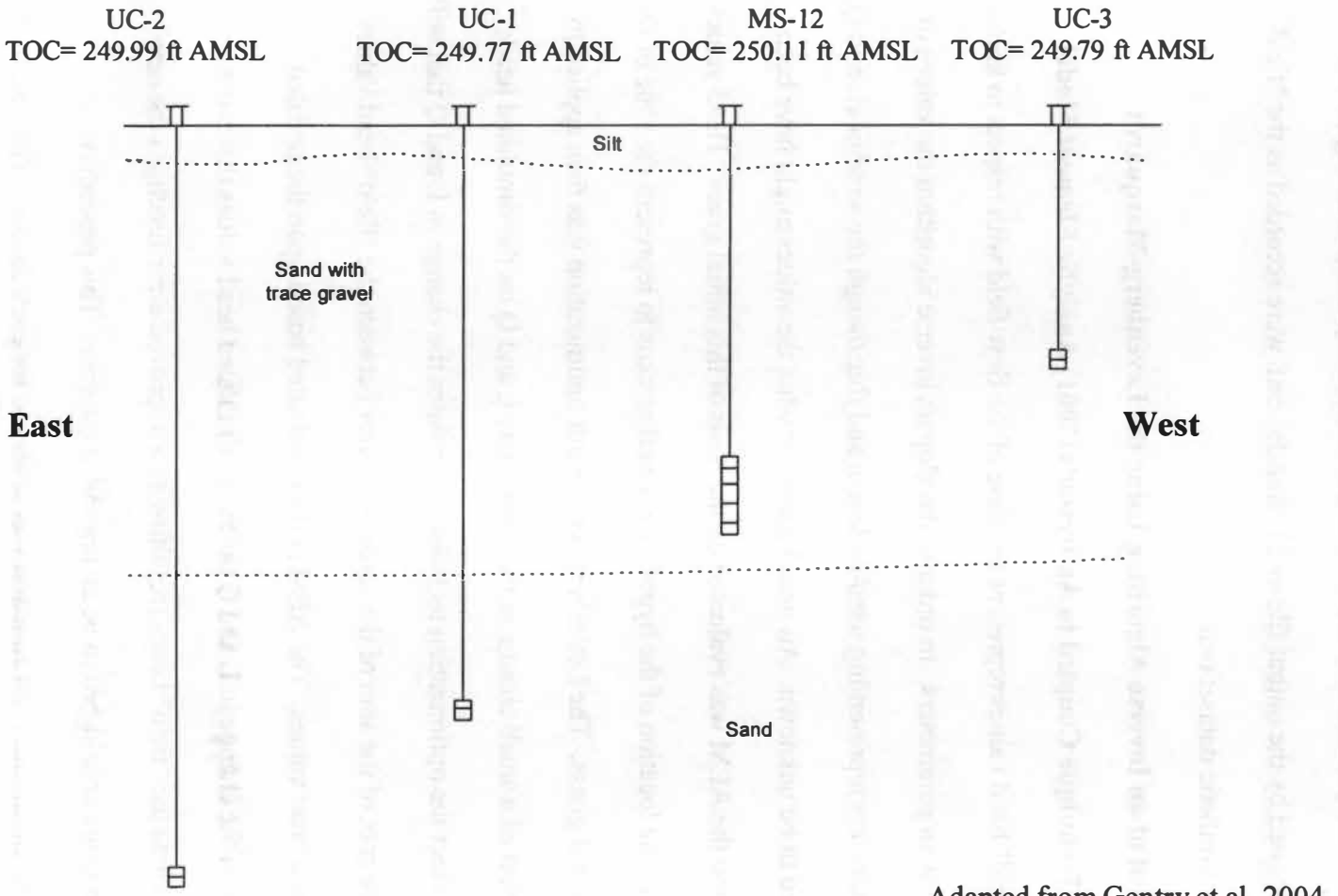

Figure 3.2. Wells Present Within the Shelby Farms Site Window
TOC: Top of Casing, The letters and numbers presented above the TOC value are the well names sighted in AwwaRF report by Gentry et al. 2004.

The flow field produced by these input parameters is presented as ***Figure 3.3***. Head values reported by the output file `well_heads.out` were recorded as the "field" head values for synthetic dataset two.

3.2 Development of an Inverse Algorithm Using the Levenberg-Marquardt Optimization Technique Coupled to Anderson's (2001) Analytic Element Model

The "field" head values represent the state of the flow field with respect to known values of the system parameters. In order to develop an inverse algorithm the values of the system parameters representing *window length* and *flux though the window* (L and Q) were considered to be unknown. An initial guess for what the values might have been was provided and the AEM was evaluated on the basis of this initial guess. Head values were recorded at the location of the hypothetical well screens to represent the state of the system at the initial guess. The Levenberg-Marquardt optimization was then applied to evaluate the effect of a small change in the parameters L and Q on the simulated heads. Based on this effect the optimization technique calculates the change in L and Q that will lower the square root of the sum of the squares of error between the "field" head values and the simulated head values. The AEM is then evaluated based upon the updated prediction. When the change in L and Q produces simulated head values that more closely approximate the "field" heads (resulting in a improved error function) the new values of L and Q are considered to be an improved estimate. This procedure was repeated until the minimum error function was achieved for each dataset. The minimum error function was achieved when the optimization technique did not produce an improved error function. This application of the Levenberg-Marquardt optimization to

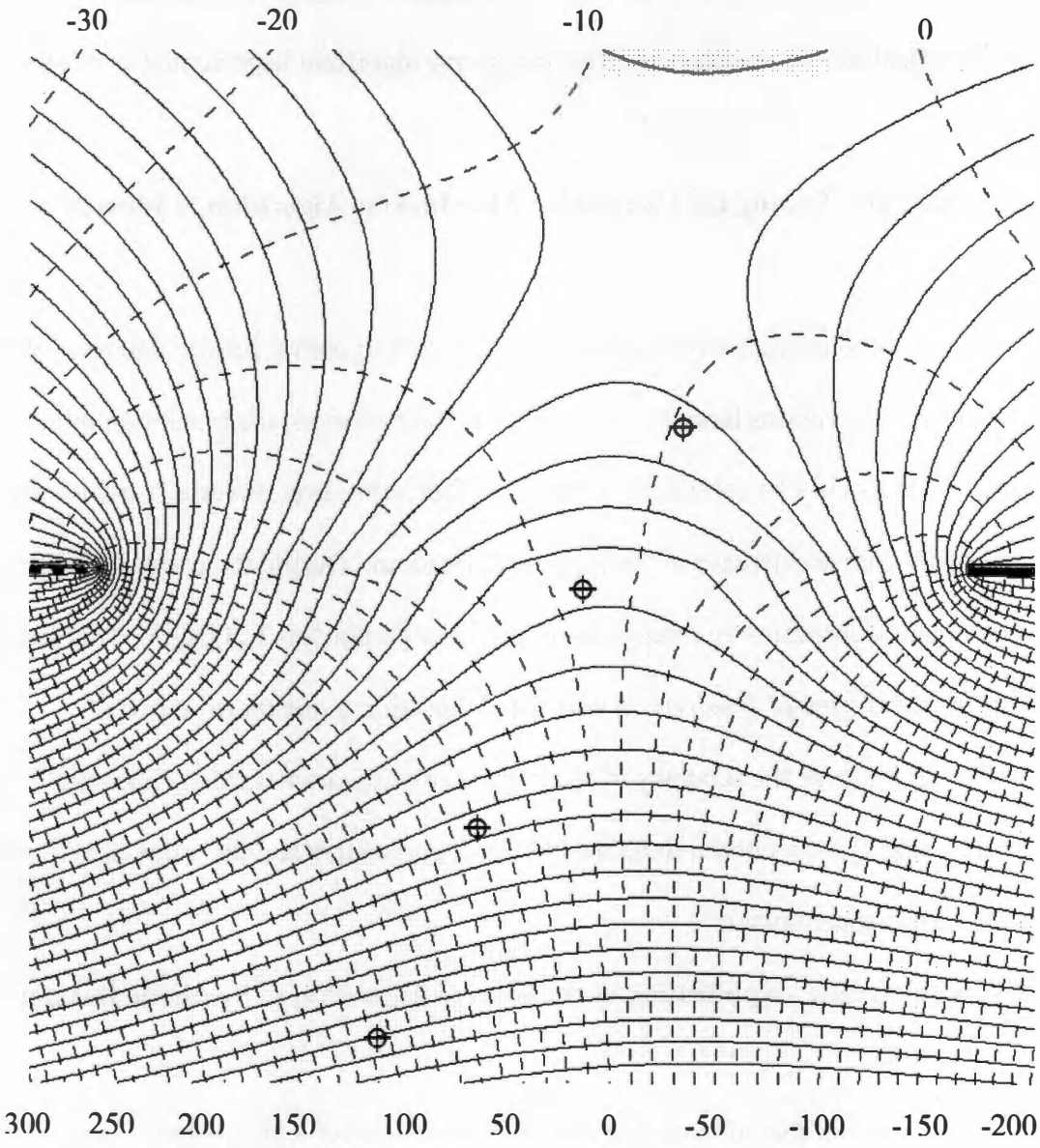

Figure 3.3 Flow Field Map of Known Parameters - Synthetic Dataset Two
This figure represents a vertical cross section through a window of unit width normal to the vertical plane. All head values are presented in feet.

L=173ft Q=113 ft^3/day

Head Contours
Flow Paths

100 ft
Scale

Location of Synthetic Data Point Collection

Anderson's 2001 AEM constitutes the inverse algorithm developed for this study. A flow chart of the calculation procedures used in the inverse algorithm is presented as ***Figure 3.4***

3.3 Experimentally Testing the Capability of the Inverse Algorithm to Identify a Solution

The Levenberg-Marquardt algorithm was applied to both synthetic datasets. With only four head observations to assess error in the inverse process, the maximum number of parameters that could be solved for inversely is four. However, inverse solutions are often improved with an increase in the degrees of freedom. During the early stages of this research the algorithm was setup to solve for three parameters L, Q, $Q^{(u)}$. This setup offered only one degree of freedom. It was noted that adding one more degree of freedom would increase the accuracy of the inverse solution dramatically. Thus the parameters L and Q were chosen to be the unknown parameters and the value of $Q^{(U)}$ was entered as a known parameter.

3.3.1 Experiment One - Application of the Inverse Algorithm to Synthetic Dataset One

The first test of the inverse algorithm was implemented with synthetic dataset one. The initial guesses of L= 193 ft and Q= 10 ft^3/day returned head values that had an error function value of E= 63.5. The initial guess values were chosen to be on the outer edge of the 100% difference range to illustrate the robust nature of the inverse technique to the analytic element model equations developed by Anderson (2001). The flow field of the initial guess was observed to have head values in the same range of those in the known flow field, as would be expected, ***Figure 3.5***.

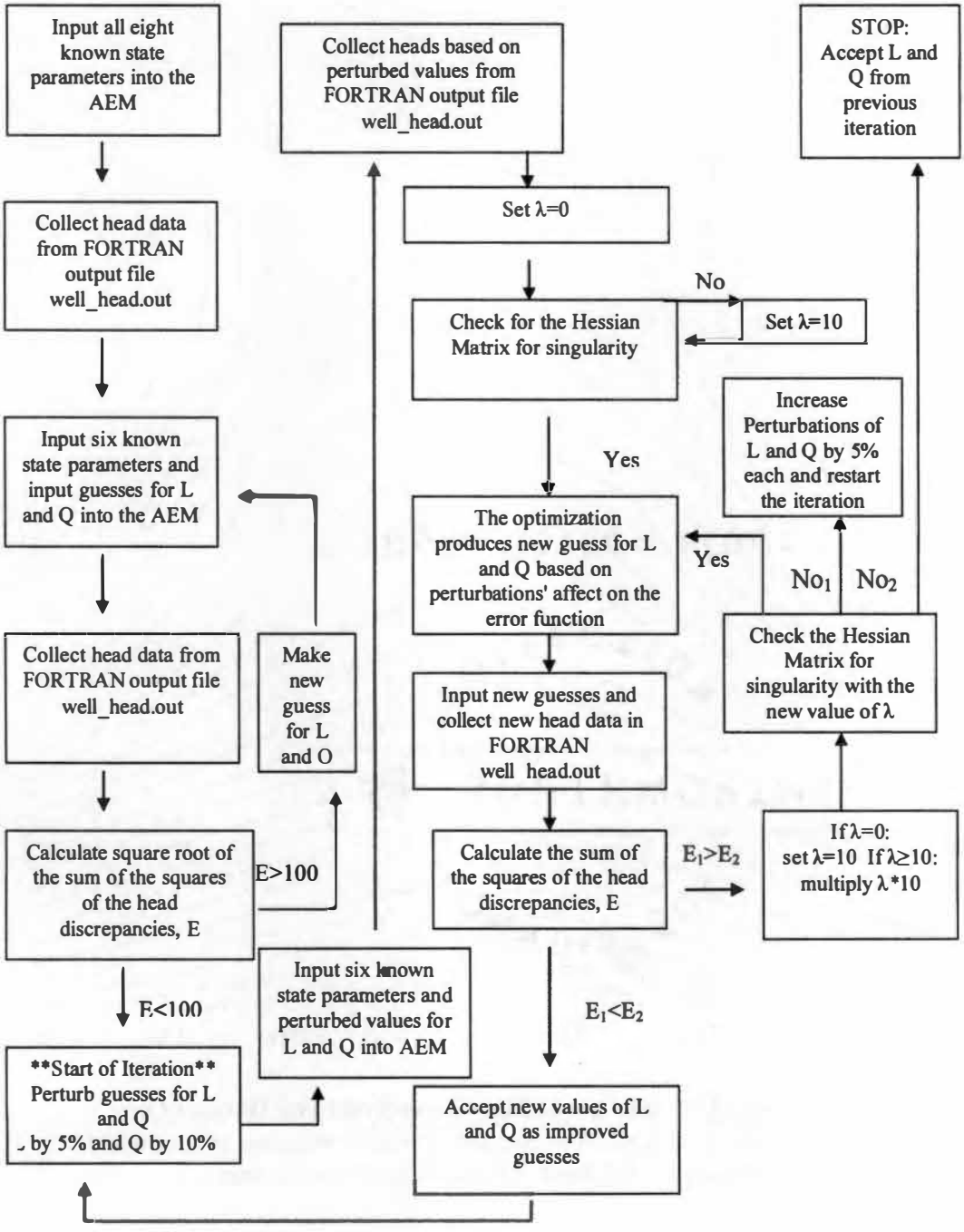

Figure 3.4 Flow Chart of the Inverse Algorithm
The subscript 1 following a condition statement such as "No" means that step is only taken once during an iteration. The subscript 2 indicates the step that is to be taken only after an iteration in which the step with the subscript 1 has been taken

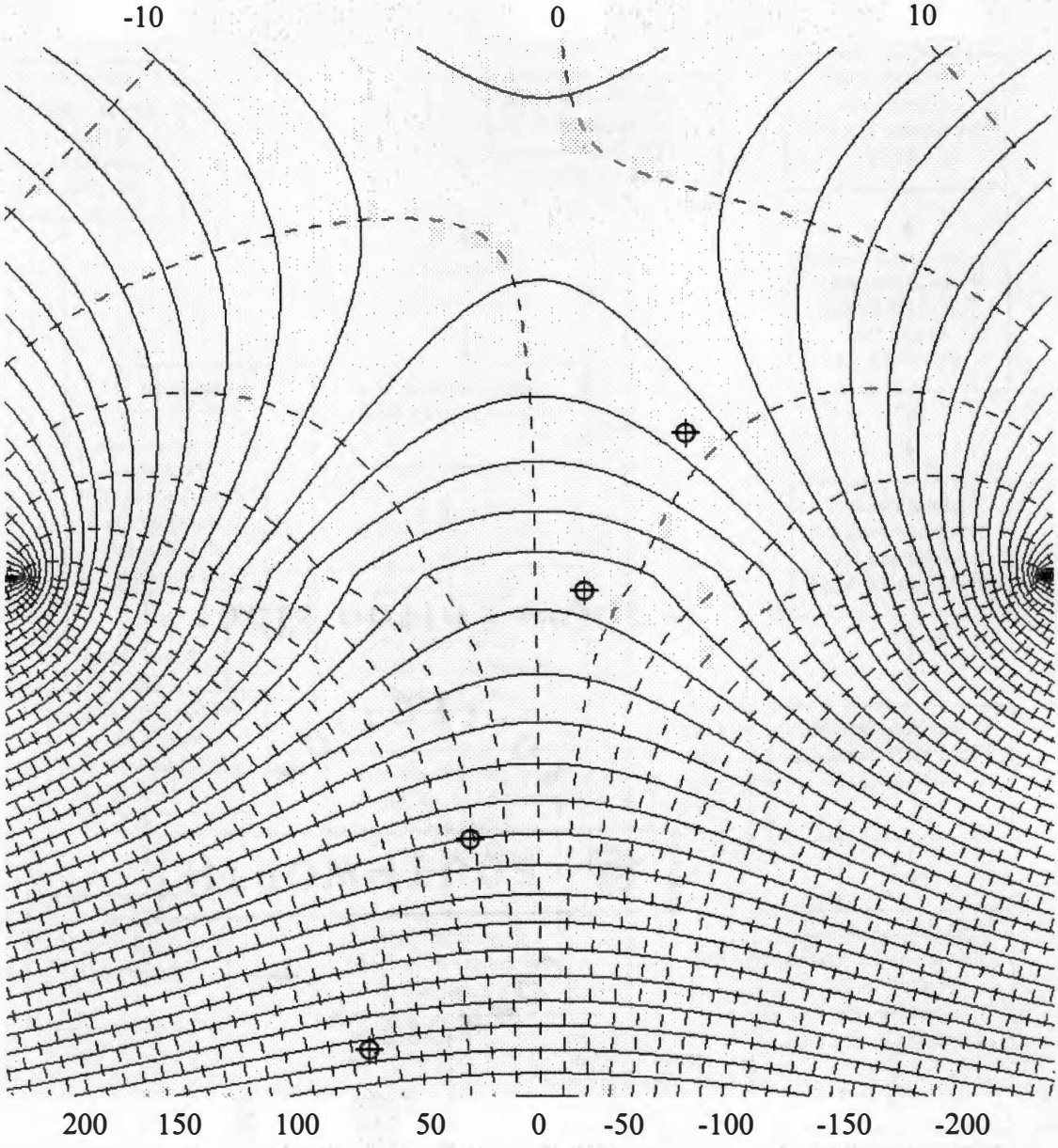

Figure 3.5 Flow Field Map of the Initial Guess-Synthetic Dataset One
This figure represents a vertical cross section through a window of unit width normal to the vertical plane. All head values are presented in feet.

The Levenberg-Marquardt inverse algorithm was applied with a 5% perturbation for the parameter representing L and a 10% perturbation for the parameter representing Q. After seventeen iterations the inverse algorithm would not produce a lower error function for any value of λ. The perturbations of L and Q were increased to 10% and 15%, respectively, in an effort to move in an observable search direction. This new perturbation produced an improved error function and iteration proceeded until the inverse algorithm could no longer produce an improved error function. This point was reached during iteration nineteen. Therefore, the values for L and Q were taken to be the solutions from iteration eighteen.

3.3.2 Experiment Two - Application of the Inverse Algorithm to Synthetic Dataset Two

Next, the inverse algorithm was applied to the second set of synthetic data. The initial guess values were L = 100 ft, Q = 200 ft^3/day. This initial guess produced an error function value of E = 78.82. The resultant flow field of the initial guess is represented as ***Figure 3.6***. Once again, values for L were perturbed by 10% and values for Q were perturbed by 5% during each iteration. In contrast to the first dataset, during the inverse calculations for the second dataset the perturbation values did not need to be adjusted. After the tenth iteration the error function could not be lowered for the any value of λ. The values of L and Q returned by the ninth iteration were accepted as the solution to the inverse problem.

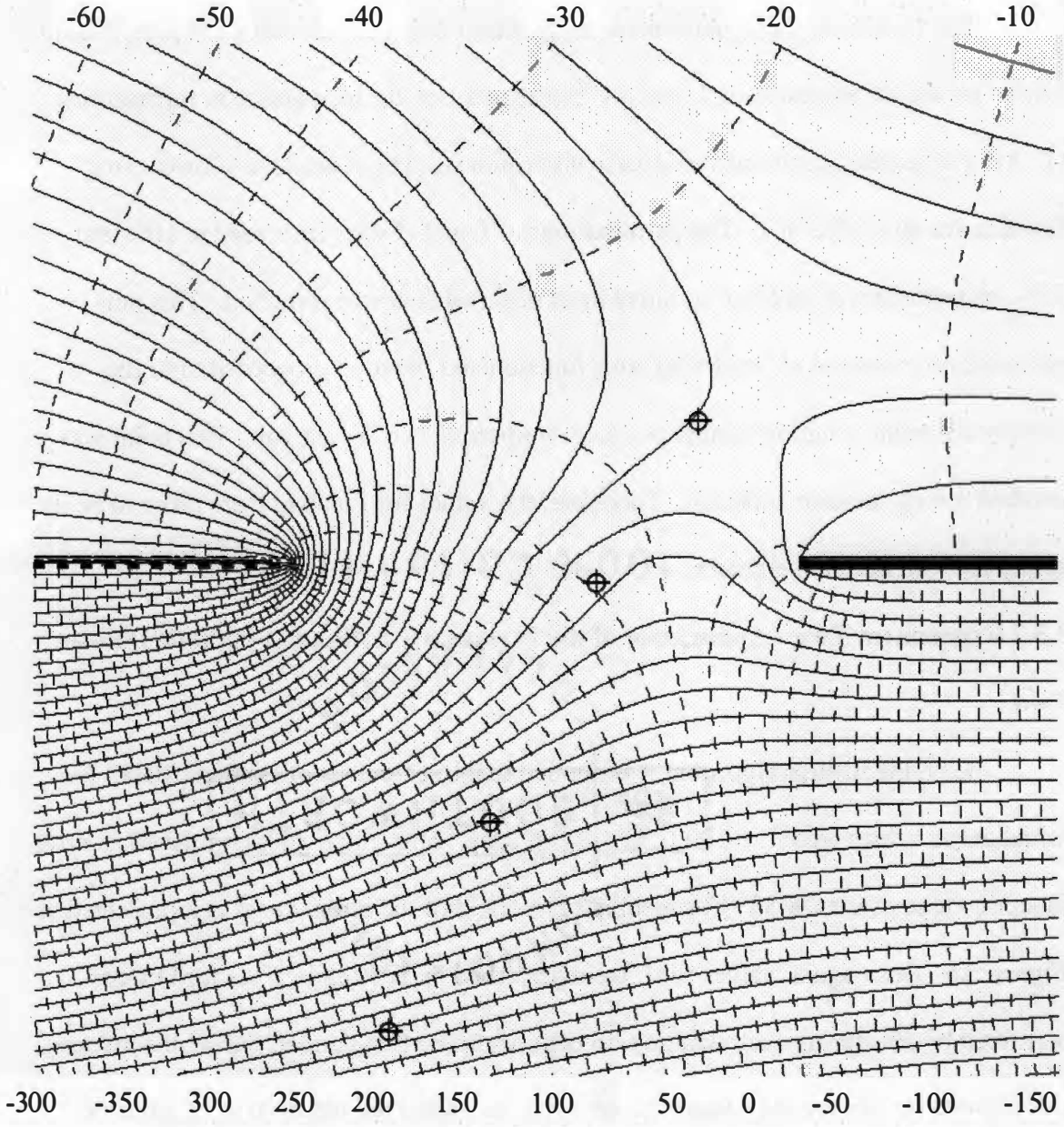

Figure 3.6 Flow Field Map of Initial Guess - Synthetic Dataset Two
This figure represents a vertical cross section through a window of unit width normal to the vertical plane. All head values are presented in feet.

L=100 ft Q=200 ft^3/day

---------- Head Contours

_____ Flow Paths

100 ft
Scale

⊕ Location of Synthetic Data Point Collection

3.3.3 Experiment Three - Test the Stability of the Inverse Algorithm

A sensitivity analysis was performed in order to establish whether or not random errors in the measurement of heads would greatly affect the ability of the inverse algorithm to predict reasonable values for L and Q. For example, small changes in the observation data could lead to large changes in predictions of L and Q. This would be an indication of an unstable inverse model. This analysis was performed on synthetic dataset one. The head values were perturbed randomly by ±5% in three separate trials (P1 - P2). ***Table 3.1*** shows the perturbed head values used in the sensitivity analysis.

3.3.4 Experiment Four - Test the Effect of Added Observation Data on the Inverse Solution

Adding head observations to define the state of the system will increase the degrees of freedom in the inverse solution. A single fixed data point was added to the synthetic datasets to illustrate the effect on the inverse solution. While it was anticipated that the added data points would improve the accuracy of the inverse solution, the best location for a new fixed data point was not known. The inverse algorithm was evaluated three separate times with the added data point in three separate locations. The three locations are illustrated in ***Figure 3.7***. Position one is located at the boundary between the two aquifers and on the edge of the window. Position two is located in the vertical center of the upper aquifer and above the window edge. Position three is located at right hand boundary of the upper aquifer.

3.4 Application of the Inverse Algorithm to the Field Test Case

The field test case chosen for inverse application of Anderson's 2001 AEM was the Shelby Farms site in Memphis, Tennessee. The site is known to contain an aquitard

Table 3.1
Head Values (ft) Used in the Sensitivity Analysis

Synthetic Well	Head P 1	P 2	P 3	True Value
1	129.68	130.01	124.12	125.67
2	55.69	54.40	54.99	53.72
3	-4.34	-4.16	-4.08	-4.25
4	-6.50	-6.56	-6.38	-6.65

Wells are counted left to right in Figure 3.6., the left most well being Well 1 and the right most well being Well 4. The notation P1 indicates perturbation trial one.

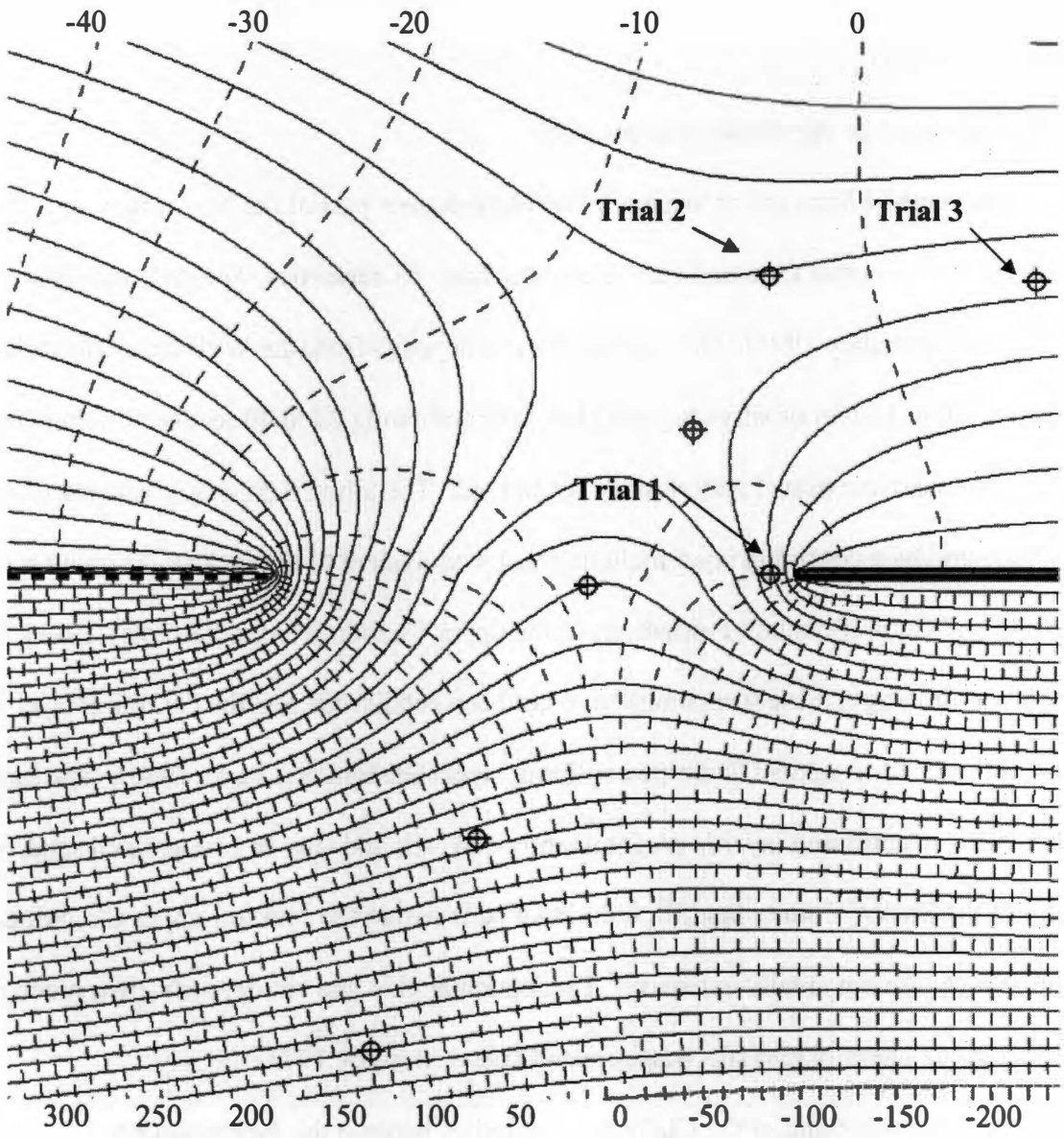

Figure 3.7 Location of Additional Synthetic Well Screens
This figure represents a vertical cross section through a window of unit width normal to the vertical plane. All head values are presented in feet.

L=100 ft Q=100ft^3/day

---------- Head Contours
_____ Flow Paths

100 ft
Scale

⊕ Location of Synthetic Data Point Collection

window and was selected to test the robust nature of the algorithm with actual filed data (Gentry et al. 2004)

3.4.1 Background on the Shelby Farms Site

The Shelby Farms site is located in the north-central part of the Mississippi embayment. It is underlain by several thousand feet of unconsolidated Cretaceous, Tertiary, and Quaternary age sediments (Bradley 1991). On site, the alluvial deposits from the Wolf River floodplain are made up of 10 to 15 feet of silty clay and clay. The following 20 to 40 feet of alluvium are composed of sand and gravel with minor clay and silt. The alluvial deposit is separated from the Memphis Sand by a confining layer including strata equivalent to the Jackson Formation and the Cockfield and Cook Mountain Formations of the upper Claiborne Group (Bradley 1991). Due to similarity in lithology, these formations have not been subdivided and the confining layer is known as the Jackson-upper Claiborne confining layer (Graham and Parks 1986). The Jackson-upper Claiborne confining layer is predominantly clay, silt and silty or fine-grained sand. In the vicinity of the Shelby County landfill, individual beds within the Jackson-upper Claiborne confining layer are not areally extensive. The lenticular clay and silt deposits often pinch out rapidly or grade laterally into silty-sand or sand layers (Bradley 1991)

The Memphis Sand of the Claiborne Group lies beneath the Jackson-upper Claiborne confining layer. The upper part of the Memphis Sand consists primarily of sand with some interbedded silt and clay deposits. The saturated portion of the Memphis Sand is what is commonly referred to as the Memphis aquifer

The occurrence of windows in the upper Claiborne aquitard is suspected to occur through erosional processes (Larsen et al. 2003; Gentry et al. 2004). Two conceptual models have been evaluated for windows in the upper Claiborne confining layer:

1. post-Claiborne paleovalley incision, and

2. erosion and sedimentation during the Claiborne sequence formation (Larsen et al. 2003; Gentry et al. 2004).

The window at the Shelby Farms site is suspected to have been formed from erosion and sedimentation from a deltaic area in the Mississippi Embayment during high sea levels (Gentry et al. 2004).

3.4.2 Application of the AEM and Inverse Algorithm to the Shelby Farms Site

In order to apply the analytic element model developed by Anderson (2001), the confining layer at the Shelby Farms Site had to be idealized. Where the confining layer exists, the thickness was considered negligible to that of the system as a whole. Thus, in the model, it exists as a one-dimensional line in the two-dimensional flow field containing the observation wells. The one-dimensional length of the window within the two-dimensional flow field was idealized as centered about the middle of the well distribution. The overlying aquifer was assumed to have a uniform thickness of 55 ft. The thickness considered of the Memphis Sands was 105 ft. An output model discritization was established to calculate the complex potential values every foot. Values of the complex potential were calculated on a grid of 160 ft by 1000 ft.

Because the locked parameters in the field test case are estimates, two parameter estimation sets were made. The first set (parameter set one) uses estimates of hydraulic conductivity based on local well pumping and estimates of aquifer flows based on USGS maps of the local potentiometric surfaces. The second set (parameter set two) uses regional values for the respective conductivities and assumes flow values in the upper and lower aquifer are negligible with respect to the flows associated with the window

feature. The inverse algorithm was applied to both parameter sets. A detailed discussion of these parameter sets is given in the following sections.

3.4.2.a Shelby Farms Parameter Set One

Locked parameter values in the initial forward modeling of the Shelby Farms site are presented below.

$$k^{(u)} = 100\frac{ft}{day} \qquad Q^{(l)} = 1.3\frac{ft^3}{day}$$
$$k^{(l)} = 9.8\frac{ft}{day} \qquad \Phi_{(0)}^{(u)} = 21923.933\frac{ft^3}{day}$$
$$Q^{(u)} = 13.92\frac{ft^3}{day} \qquad b = 1\,ft$$

The value entered for the parameter $k^{(u)}$ was selected based upon recent studies at the site that determined the hydraulic conductivity in the upper aquifer was 100 ft/day (Gentry et al. 2004). The value entered for parameter $k^{(l)}$ is the vertically weighted average of hydraulic conductivities reported by Gentry et al. (2004) for wells UC-2 and UC-1, ***Figure 3.2***. The parameter $Q^{(u)}$ and $Q^{(l)}$ were calculated with the following equation relating volumetric flow to hydraulic conductivity, aquifer thickness, and hydraulic head in a confined system.

$$Q = kH\frac{dh}{ds}$$

k= hydraulic conductivity

H= aquifer thickness,

$\frac{dh}{ds}$ = change in head per linear distance in the direction of flow

Both the upper and lower aquifers were assumed to have the behavior of confined aquifers. The values of dh/ds in the upper and lower aquifer were approximated from historical water table data for the Shelby Farms Site (Parks and Mericki 1992).

The value of $\Phi_{(o)}^{(u)}$ is a calculated parameter using the following relationship (Strack 1989):

$$\Phi_{(0)}^{(u)} = k_{(u)} b \varphi$$

$k_{(0)}$= hydraulic conductivity at the origin

b= aquifer width normal to the z plane

φ= hydraulic head along the imaginary axis (field observation)

The variable $\Phi_{(o)}^{(u)}$ serves as a scaling variable for the system and was estimated at a location between UC-1 and MS-12.

The six known parameter values were entered into the forward model with an initial guess of L= 500 ft and Q= -500 ft^3/day. This initial guess produced an error function of E=8.5. The flow field of the initial guess is presented as ***Figure 3.8***.

3.4.2.b Shelby Farms Parameter Set Two

In parameter set two the specific parameters that were reconsidered were the hydraulic conductivities and the values for flow in the upper and lower aquifers. The value entered for hydraulic conductivity in the upper aquifer was considered a realistic value for the region. However, the value of hydraulic conductivity entered for the lower aquifer was considered to be inconsistent with regional values and more likely represents a very localized value. A new value of 40 ft/day was entered as the hydraulic conductivity in the lower aquifer. This value was considered to be more representative

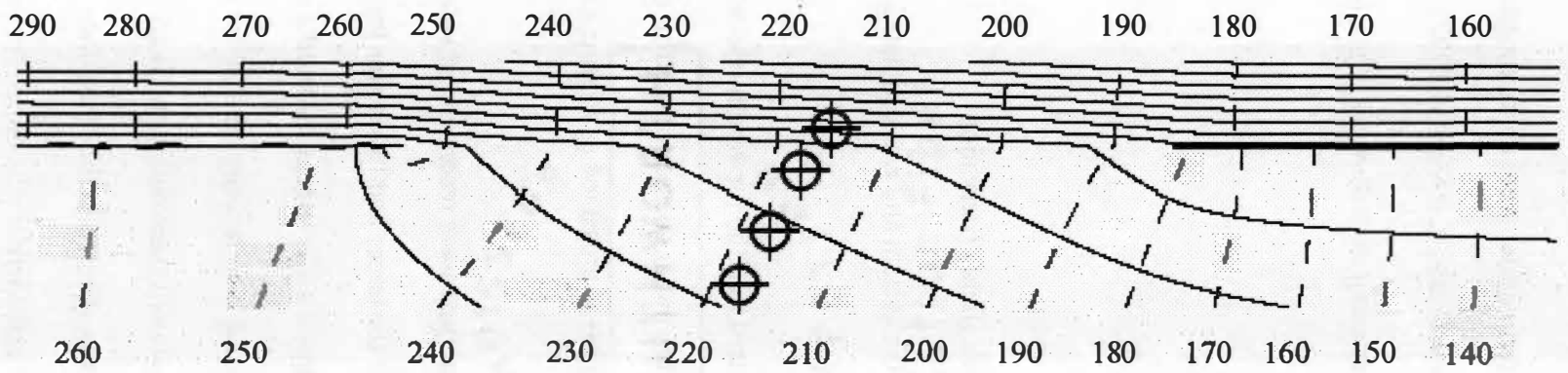

Dataset 7/12/2004

Figure 3.8 Flow Field Map of the Initial Guess - Parameter Set One

This figure represents a vertical cross section through a window of unit width normal to the vertical plane. All head values are presented in feet. This flow field is considered to be an unrealistic depiction of the Shelby Farms Site due to inaccuracies in estimating the flows in the upper and lower aquifers

L=500 ft Q=-500 ft^3/day

---------- Head Contours

_____ Flow Paths

500 ft

Scale

⊕ Location of Synthetic Data Point Collection

on a regional scale. The values for flow in the upper aquifer and flow in the lower aquifer were entered as 0 with the assumption that flows in the vicinity are dictated more by the presence of the window than by regional flow magnitudes.

These new assumptions, shown below, provided a much more realistic prediction of heads on the boundaries of the model.

$$k^{(u)} = 100\frac{ft}{day} \qquad Q^{(l)} = 0.0\frac{ft^3}{day}$$

$$k^{(l)} = 40\frac{ft}{day} \qquad \Phi^{(u)}_{(0)} = 21923.933\frac{ft^3}{day}$$

$$Q^{(u)} = 0.0\frac{ft^3}{day} \qquad b = 1\,ft$$

The values of the new initial guess of L=500 ft and Q=-500 ft^3/day were used once again. These initial guesses produced a very low error function of E= 3.9. The flow field produced by the AEM for parameter set two is presented in ***Figure 3.9***.

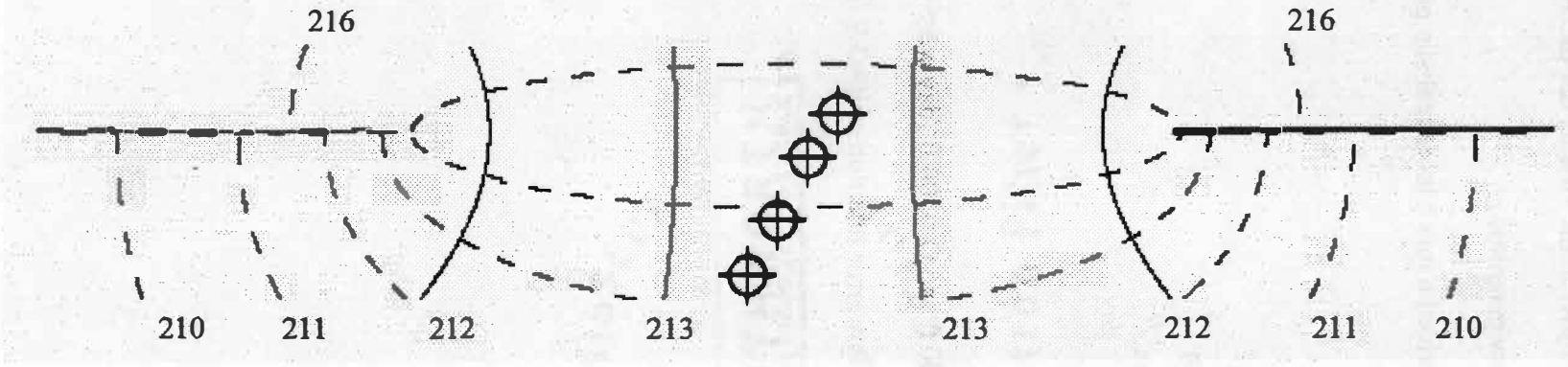

Dataset 7/12/2004

Figure 3.9 Flow Field Map of the Shelby Farms Initial Guess - Parameter Set Two

This figure represents a vertical cross section through a window of unit width normal to the vertical plane. All head values are presented in feet.

L=500 ft Q=-500 ft^3/day

---------- Head Contours

_____ Flow Paths

500 ft

Scale

⊕ Location of Synthetic Data Point Collection

4 Results

4.1 Results from the Synthetic Data Experiments

4.1.1 Results from the Application of the Inverse Algorithm to Synthetic Dataset One (Exp One)

The inverse algorithm produced the values L = 118.8 ft, and Q= 112.2 ft^3/day. The calculation of the forward model with these input parameters produced a final error function of E= 3.6. The values of L and Q, as well as the resulting heads calculated at the synthetic well screens, for each iteration are presented in ***Table 4.1***. As stated previously, the true values of L and Q were known to be L = 100 ft, Q = 100 ft^3/day. A graph of the values of L and Q from ***Table 4.1*** verses the number of iterations is presented as ***Figure 4.1***. A graph of the error column from ***Table 4.1*** verses the number of iterations is presented as ***Figure 4.2***. The flow field mapping of the inverse solution is presented as ***Figure 4.3***.

4.1.2 Results from the Application of the Inverse Algorithm to Synthetic Dataset Two (Exp Two)

The values produced by the inverse algorithm for synthetic dataset 2 were L= 192.3 ft and Q= 127.7 ft^3/day. The error function value associated with this solution is E= 2.0. A summary of values calculated for each iteration of the inverse procedure is presented as ***Table 4.2***. The true values for L and Q were known to be L= 173 ft and Q= 113 ft^3/day. ***Figure 4.4*** illustrates the convergence of L and Q from the initial guess to final values calculated by the inverse algorithm. A graph illustrating the decline in error during the iterative process is presented as ***Figure 4.5***. The flow field mapping

Table 4.1

Summery of Values in Each Iteration of the Inverse Algorithm - Dataset One

Iteration	L (ft)	Q (ft^3/day)	h1(ft)	h2 (ft)	h3 (ft)	h4 (ft)	lambda	E
0	193	10	71.85	19.9	-4.57	-5.62	*	63.57
1	191.9	11.1	72.35	20.15	-4.56	-5.62	1.00E+01	63.02
2	190.6	12.4	72.9	20.42	-4.56	-5.62	1.00E+01	62.4
3	189.1	13.9	73.54	20.75	-4.55	-5.62	1.00E+01	61.69
4	187.5	15.5	74.28	21.12	-4.54	-5.62	1.00E+01	60.87
5	185.6	17.4	76.06	22.03	-4.52	-5.63	1.00E+01	58.88
6	183.3	19.7	76.15	22.07	-4.52	-5.63	1.00E+01	58.78
7	180.8	22.2	77.33	22.68	-4.51	-5.63	1.00E+01	57.46
8	177.8	25.2	78.75	23.42	-4.49	-5.64	1.00E+01	55.87
9	177.8	29.2	79.89	24.09	-4.47	-5.82	0.00E+00	54.54
10	173.4	33.6	82.05	25.22	-4.44	-5.83	1.00E+01	52.11
11	167.8	39.2	84.89	26.74	-4.41	-5.86	1.00E+01	48.91
12	160.3	46.7	88.88	28.9	-4.36	-5.9	1.00E+01	44.39
13	152.3	54.7	93.36	31.4	-4.3	-5.95	0.00E+00	39.27
14	152.3	58.7	94.65	32.17	-4.27	-6.16	0.00E+00	37.78
15	126.8	84.2	111.21	41.97	-4.03	-6.58	1.00E+01	18.64
16	126.8	92.2	111.99	42.44	-3.99	-6.9	0.00E+00	17.73
17	126.8	96.2	115.68	44.7	-3.91	-7.33	0.00E+00	13.48
18	**118.8**	**112.2**	124.95	50.52	-3.72	-8.15	0.00E+00	3.64
19	129.7	101.3	116.86	45.4	-3.86	-7.76	1.00E+14	12.18

The values of L and Q identified by the inverse algorithm are in bold at iteration eighteen. The true values are L=100 ft and Q= 100 ft^3/day. Wells are counted left to right in ***Figure 3.6.***

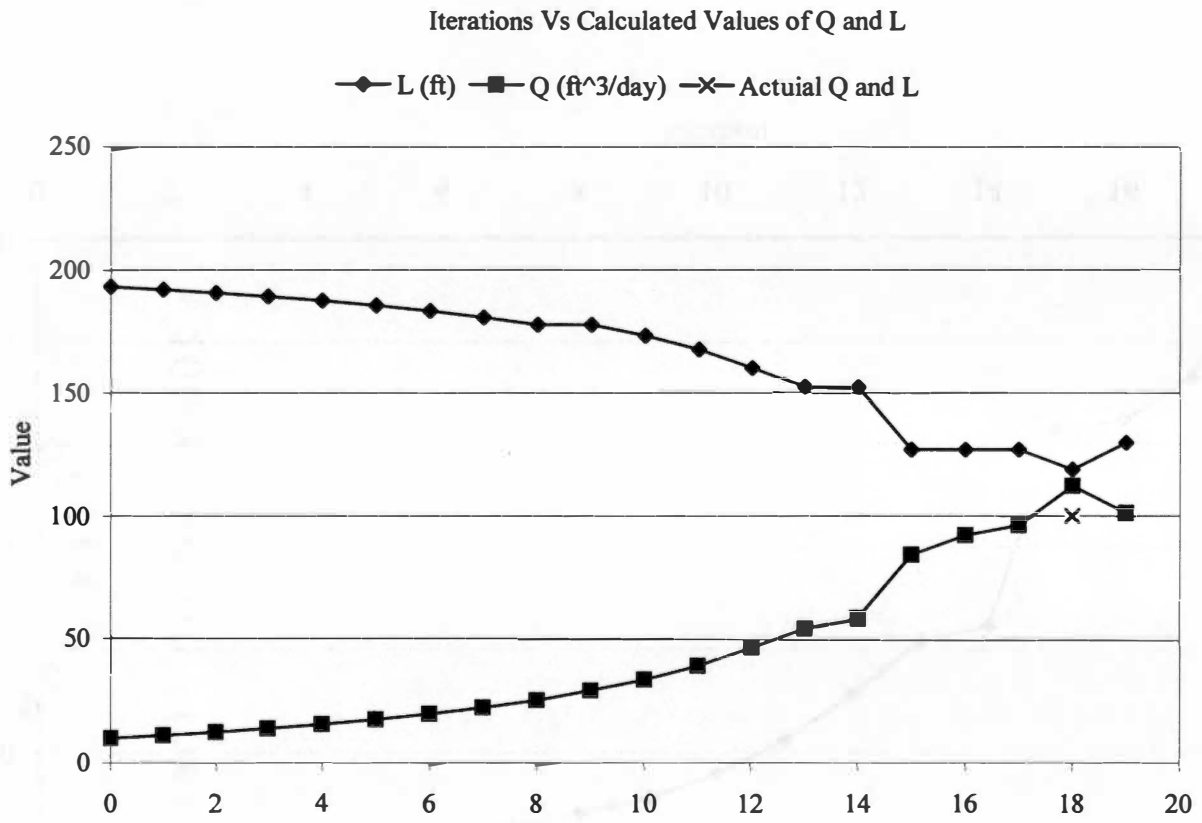

Figure 4.1 Convergence of L and Q to the Final Values Calculated by the Inverse Algorithm - Synthetic Dataset One

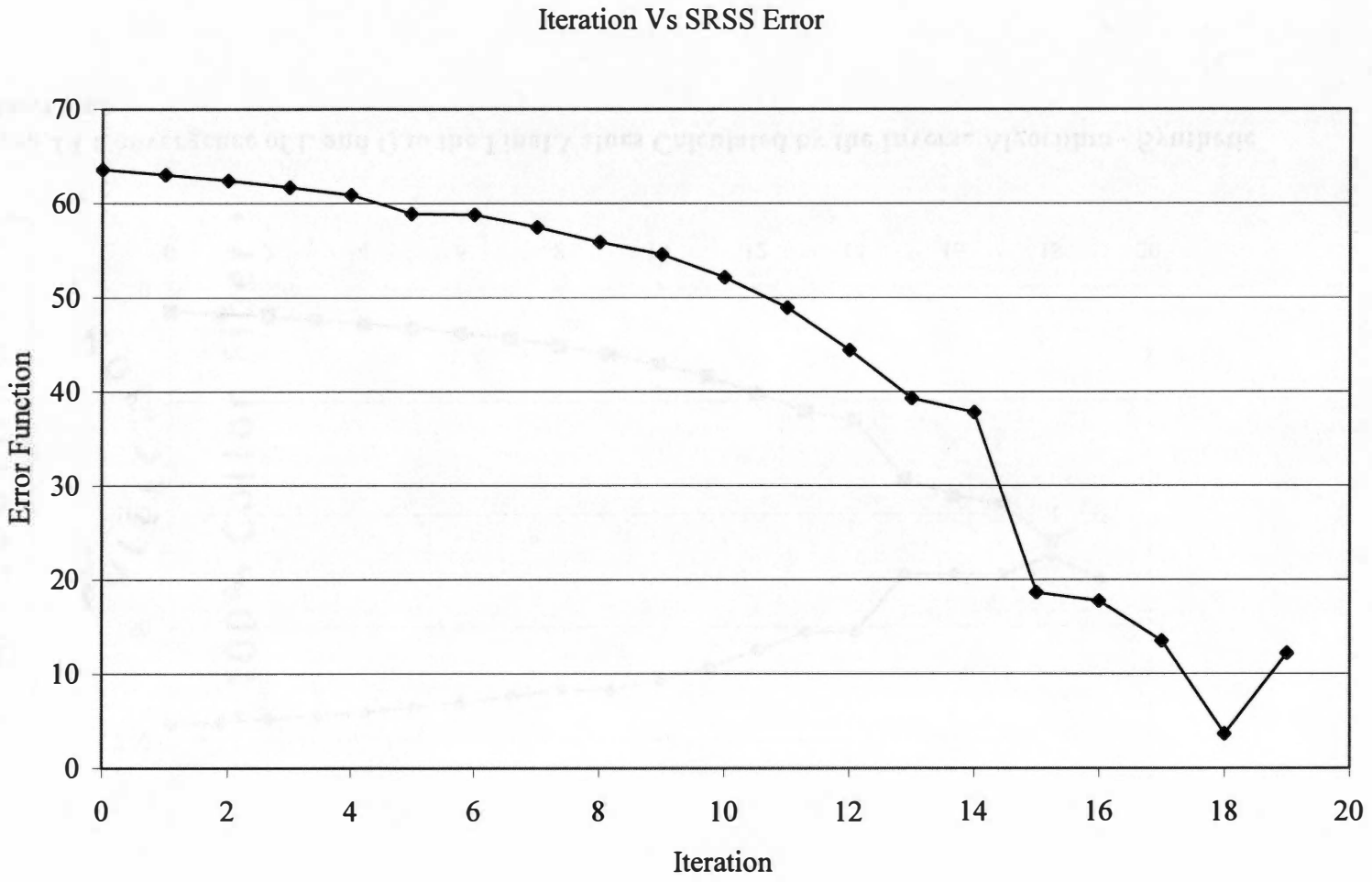

Figure 4.2 Steady Declines in the Error Function With Each Iteration - Synthetic Dataset One

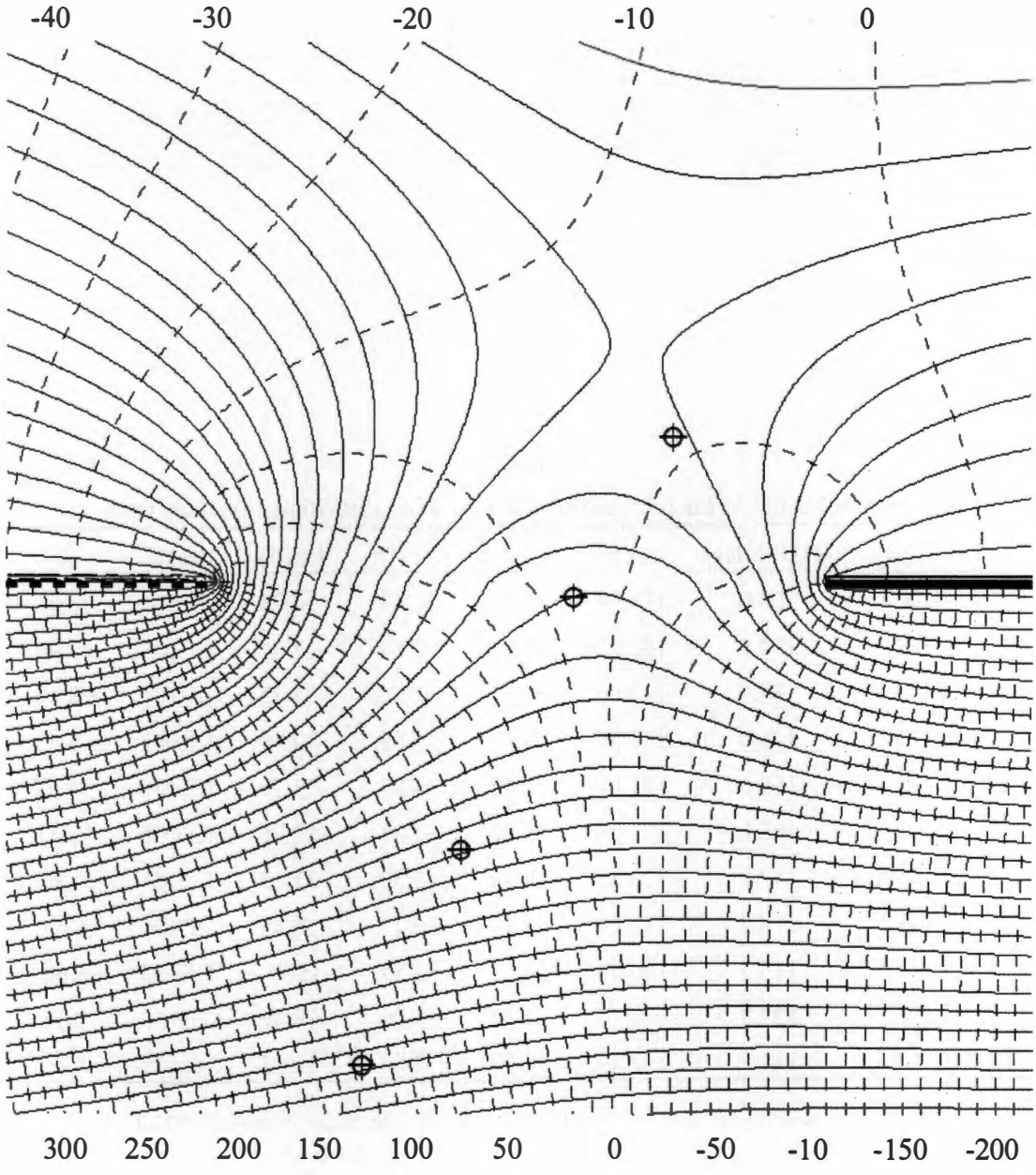

Figure 4.3 Flow Field Map of the Inverse Solution - Synthetic Dataset One
This figure represents a vertical cross section through a window of unit width normal to the vertical plane. All head values are presented in feet.

L=118.8 ft Q=112.2 ft^3/day

---------- Head Contours
———————— Flow Paths

100 ft
Scale

⊕ Location of Synthetic Data Point Collection

Table 4.2

Summery of Values in Each Iteration of the Inverse Algorithm - Dataset Two

Iteration	L (ft)	Q (ft^3/day)	h1 (ft)	h2 (ft)	h3 (ft)	h4 (ft)	lambda	E
0	100.0	200.0	171.97	80.96	-2.49	-14.76	*	78.82
1	107.1	192.9	163.92	75.30	-2.69	-13.91	1.E+01	68.96
2	115.1	184.9	155.60	69.63	-2.89	-13.13	1.E+01	58.87
3	124.1	175.9	146.91	63.89	-3.08	-12.40	1.E+01	48.43
4	134.4	165.6	137.81	58.08	-3.26	-11.73	1.E+01	37.62
5	142.4	165.6	133.98	55.67	-3.31	-11.75	0.E+00	33.11
6	155.8	152.2	123.65	49.48	-3.50	-11.12	1.E+01	21.05
7	173.3	134.7	111.19	42.34	-3.71	-10.40	1.E+01	6.69
8	192.3	115.7	100.48	36.51	-3.87	-9.97	1.E+15	5.60
9	**192.3**	**127.7**	103.79	38.42	-3.79	-10.47	0.E+00	2.04
10	192.3	121.5	100.24	36.53	-3.84	-10.31	1.E+14	5.85

The values of L and Q identified by the inverse algorithm are in bold at iteration nine. The true values are L=173 ft and Q= 113 ft^3/day. Wells are counted left to right in ***Figure 3.6***.

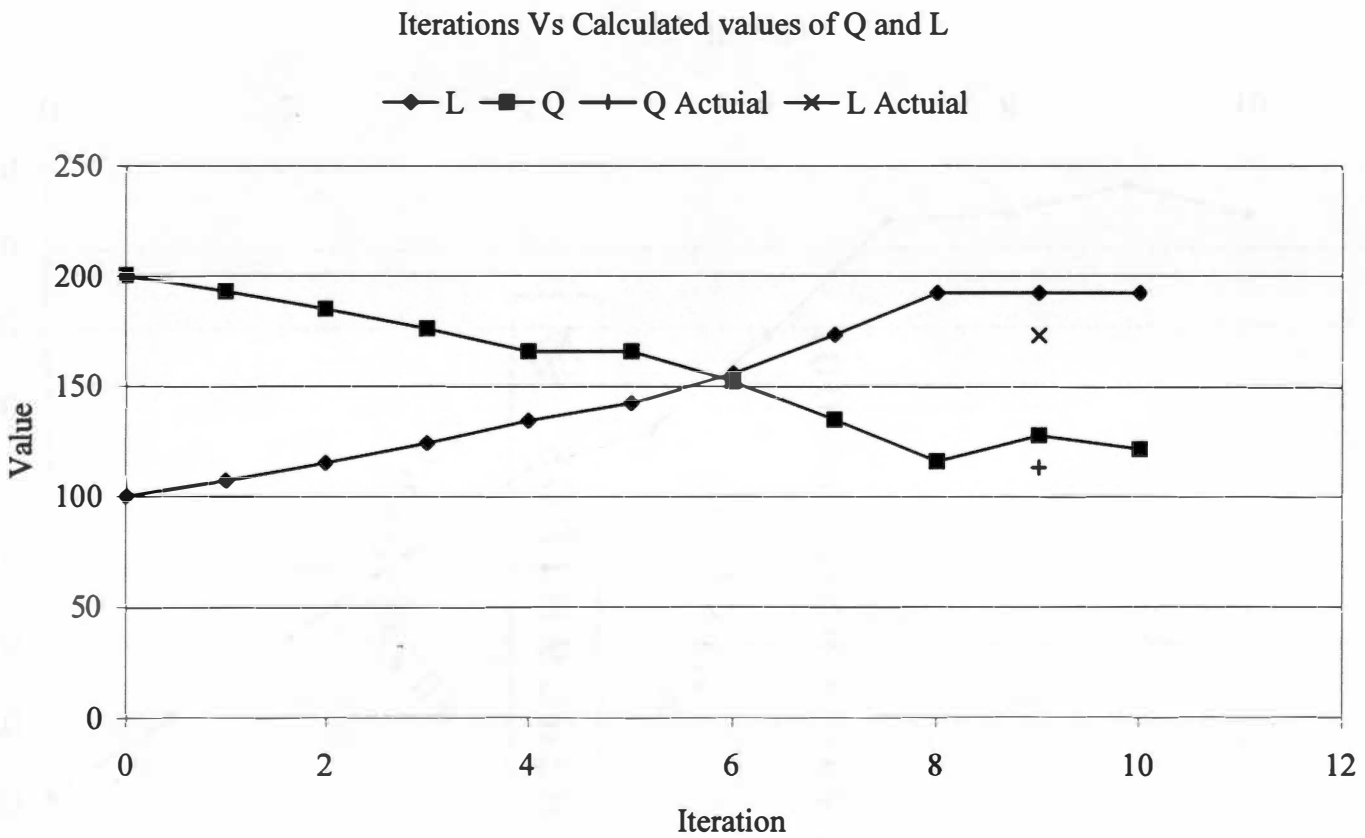

Figure 4.4 Convergence of L and Q to the Final Values Calculated by the Inverse Algorithm - Synthetic Dataset Two

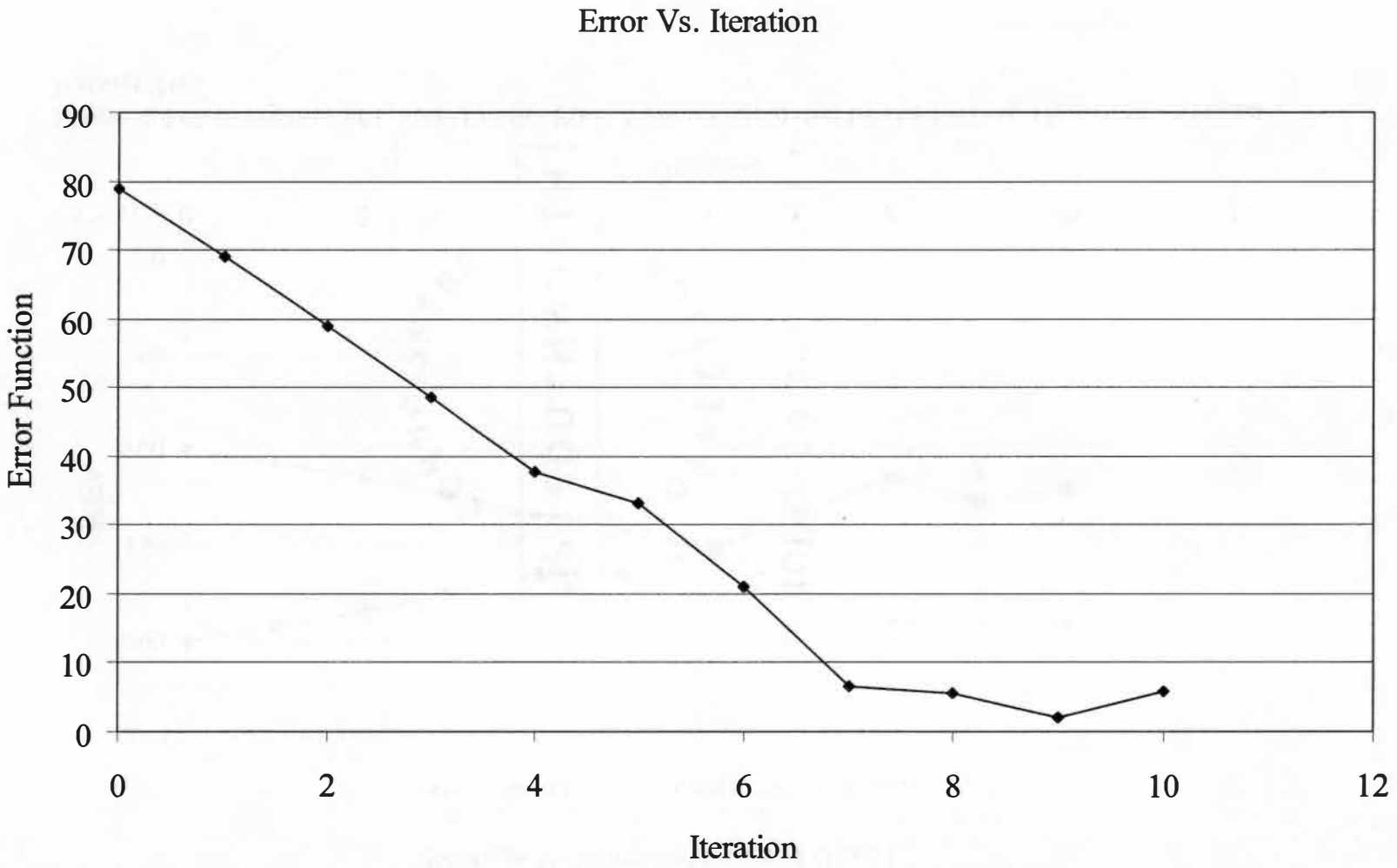

Figure 4.5 Steady Declines in the Error Function With Each Iteration - Synthetic Dataset Two

produced by the input of parameters calculated by the inverse procedure is presented as ***Figure 4.6***.

4.1.3 Stability Test Results With Dataset One (Exp Three)

The inverse algorithm was run on the three perturbed "field' head datasets, P1-P3. The results of the inverse algorithm for the three perturbed "field" head datasets are presented in ***Table 4.3***.

4.1.4 Results of Added Head Observations (Exp Four)

The inverse algorithm was run for each trial of an added synthetic well observation (T1 - T2). ***Table 4.4*** is a summery of values of L and Q identified for each trial. ***Table 4.5*** shows the percent difference between the calculated values and the known values of L and Q for each trial. Locations of the synthetic well screen in each trial can be observed in ***Figure 3.7.***

4.2 Results from the Application of the AEM and Inverse Algorithm to the Field Test Case

The inverse algorithm was run on both parameter set one and two. The parameter set that provided the most realistic flow field realization was chosen as the parameter set that best represents the site characteristics. Additional head data taken on two separate occasions was then applied to the chosen parameter set and the inverse algorithm.

4.2.1 Results from the Inverse Algorithm Application to Shelby Farms -Parameter Set One

With the initial guesses of L=500 ft and Q= -500 ft^3/day, the inverse algorithm was run for seventeen iterations. The error function associated with the initial guess was

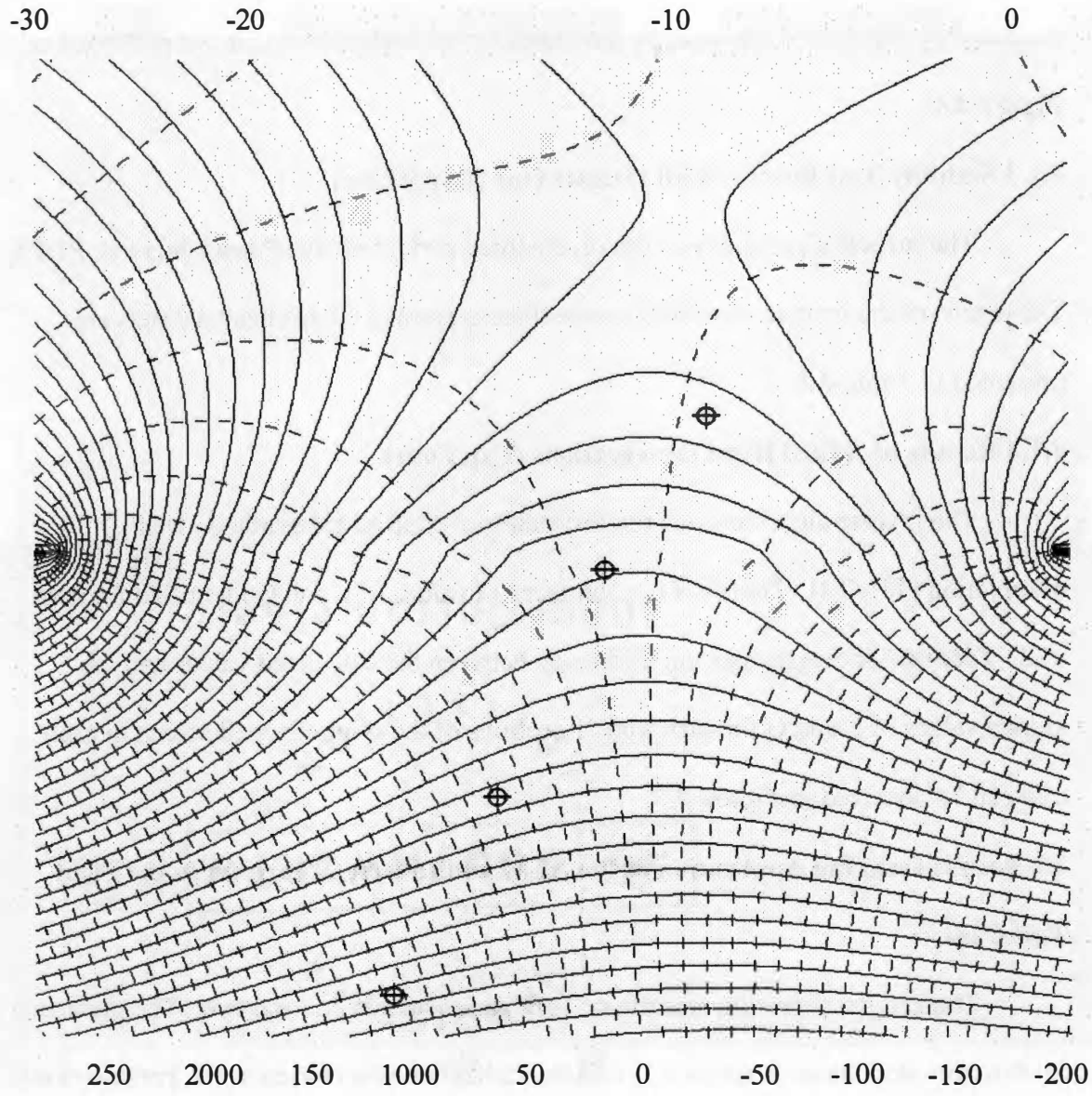

Figure 4.6 Flow Field Map of the Inverse Solution - Synthetic Dataset Two
This figure represents a vertical cross section through a window of unit width normal to the vertical plane. All head values are presented in feet.

L=192.3 ft Q=127.7 ft^3/day

---------- Head Contours

_____ Flow Paths

100 ft

Scale

⊕ Location of Synthetic Data Point Collection

Table 4.3
Results From the Sensitivity Analysis

	P 1	P 2	P 3
L (ft)	103.7	111.6	109.9
Q (ft^3/sec)	99.0	105.4	95.0

Table 4.4

Summery of Inverse Solutions With an Added Observation

	Trial 1	Trial 2	Trial 3	Known
L (ft)	112.0	101.8	111.9	100.0
Q (ft^3/day)	93.0	96.2	100.1	100.0
E	9.7	3.0	6.3	n/a

Table 4.5
Percent Deviation from the Known Values
With an Added Observation Point

	Trial 1	Trial 2	Trial 3
L	12.0%	1.8%	11.9%
Q	7.0%	3.8%	0.1%

E=7.1. The values calculated by the algorithm were L= 839.3 ft and Q= -983.3 ft^3/day. The error function calculated for these numbers was E= 6.9. The flow field calculated by the application of parameter set one to the inverse algorithm is presented as ***Figure 4.7***.

4.2.2 Results from the Inverse Algorithm Application to Shelby Farms - Parameter Set Two

The same initial guess of L=500 ft and Q= -500ft^3/day was entered in concert with Parameter Set Two. The initial error function was E= 4.0. The inverse algorithm was only run for two iterations before an improved error function could not be obtained. The values of L=530.9 ft and Q= -594.9 ft^3/day were calculated with an error function of E=3.8. The flow field calculated by the application of parameter set two to the inverse algorithm is presented as ***Figure 4.8***.

4.2.3 Additional Results from the Inverse Algorithm Application to Shelby Farms - Parameter Set Two

Three sets of head measurements exist for the Shelby Farms Site, ***Table 4.6***. Because the flow field calculated by the inverse algorithm using parameters set two contains realistic values for heads near the model boundaries, the additional head measurements were applied to the inverse algorithm using parameter set two. Both of the additional datasets required two iterations with the inverse algorithm before an improved error function was achieved. The calculated values for L and Q, based on the three separate sets of wellhead data, are presented in ***Table 4.7***.

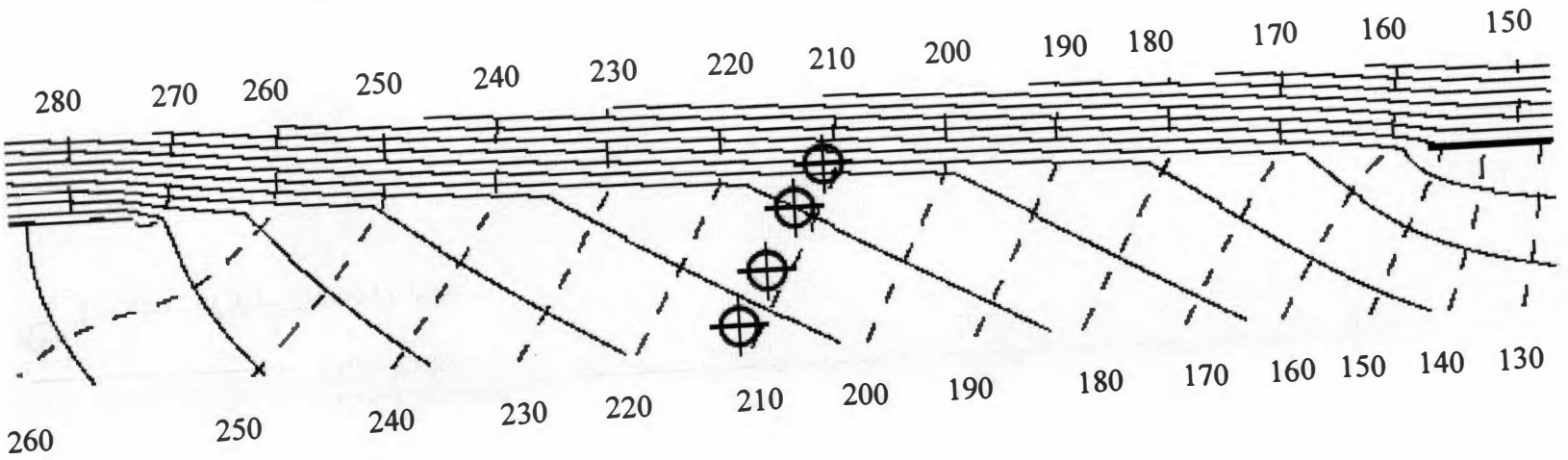

Dataset 7/12/2004

Figure 4.7 Flow Field Map of Inverse Solution at Shelby Farms - Parameter Set One

This figure represents a vertical cross section through a window of unit width normal to the vertical plane. All head values are presented in feet.

L=839.3 ft Q=-983.3 ft^3/day

---------- Head Contours

_____ Flow Paths

⊕ Location of Well-Screen Center

500 ft

Scale

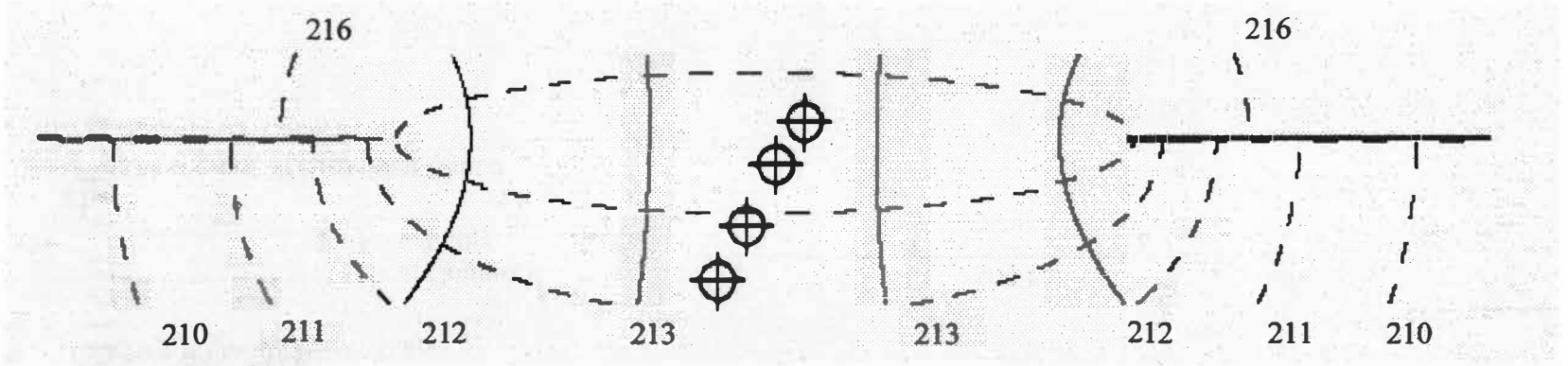

Dataset 7/12/2004

Figure 4.8 Flow Field Map of Inverse Solution at Shelby Farms - Parameter Set One

This figure represents a vertical cross section through a window of unit width normal to the vertical plane. All head values are presented in feet.

L=530.9 ft Q=-594.9 ft^3/day

---------- Head Contours

———— Flow Paths

⊕ Location of Well-Screen Center

500 ft

Scale

Table 4.6

Summary of Shelby Farms Head Measurements (ft)

Wells	7/12/2004	11/14/2002	5/17/2002
UC-2	108.68	107.82	108.39
UC-1	79.91	78.06	78.07
MS-12	41.67	38.72	38.55
UC-3	12.6	13.02	12.55

Table 4.7
Results of the Inverse Application of Anderson's AEM to the Shelby Farms Site

	7/12/2004	11/14/2002	5/17/2002	Average
L (ft)	530.90	497.80	548.00	525.57
Q (ft^3/day)	-594.90	-561.80	-564.00	-573.57
E final	3.80	2.90	2.47	3.06
E initial	3.96	7.09	2.5	4.52

5 Discussion of Results

5.1 Discussion of Synthetic Dataset Results

5.1.1 Discussion of Synthetic Dataset One Results

The results of experiment one illustrate the inverse algorithm's ability to identify values for L and Q (***Table 4.1***) that are within 20% of the true values of L and Q that produced the "field" head data. This indicates that while there is some inherent error involved in the application of this technique, the algorithm will converge to a solution that is a meaningful improvement over the initial guess. ***Figure 4.2*** shows the steady decline in the error function to the lowest achievable error at iteration eighteen. Typical behavior for gradient based techniques is observed at data point nineteen, where the solution will begin to diverge since an improved estimate of L and Q could not be made for any value of λ. The flow-chart in ***Figure 3.4*** provides an understanding of the iterative process by which the algorithm is considered to have arrived at the most improved solution. From the initial guess, the search algorithm progresses iteratively to a sequent improved solution, and ***Figure 4.8*** shows graphically how the values of L and Q changed during their convergence. The rate of convergence to an optimum solution is seen to be similar for both parameters L and Q. The convergence to an optimum solution might be considered slow with this algorithm but it is steady and stable when applied to data that is free of noise.

5.1.2 Discussion of Synthetic Dataset Two Results

The results from experiment two reinforce the results of the first experiment and indicate the robust nature of the inverse algorithm. The results of experiment two also illustrate the inverse algorithm's ability to identify values for L and Q (***Table 4.2***) that are

within 20% of actual values of L and Q associated with the "field" heads. Once again, in light of the inherent error, the algorithm converged on a meaningful improvement over the initial guess in a sequential fashion, until the algorithm could no longer identify a better search path. The steady decline in the error function to the lowest achievable error at iteration nine is observable in ***Figure 4.6***. A similar convergence pattern is identified with experiment two and the convergence of the algorithm from the initial guess values of L and Q to values that are with in 20% of the known values is seen in ***Figure 4.7***. This illustrates the ability of the algorithm to converge slowly but steadily to identify a unique solution irrespective of the relative values of L and Q and their magnitude.

5.2 Discussion of Stability Test Results

The ±5% perturbation of the head data in experiment three had a negligible affect on the ability of the inverse algorithm to produce a solution. The results summarized in ***Table 4.3*** show that even with the perturbation of the "field" heads, the algorithm still converged to values of L and Q that were within 20% of the true values. This illustrates that the inverse algorithm is stable with respect to the heads as state observations. If random perturbation caused large discrepancies in the values calculated for L and Q the inverse algorithm would have been considered unstable and therefore not practical for use in a field case where noise in the data is a possibility.

5.3 Discussion of the Effect of Added Head Observations

The added observation points in trials one through three (T1 -T3) provided some interesting insight as to where the best place to add an observation point in this system would be. Each added observation provided improved estimates of L and Q. However, trial two seemed to provide the most improved estimate of L and Q, ***Table 4.5***. Though

trial one provided an improved estimate, the observation in trial one is located in an area of the window where the head gradient is relatively high. This is potentially the reason that the added observation at this point did not give the largest improvement in a final estimate of both L and Q. The observation point used in trial three is located the furthest from the window. The larger overall error can most likely attributed to this fact.

It was observed during experiment four that an additional observation point outside the center of the window will improve the estimate of L and Q calculated by the inverse algorithm. The error function for each trial was higher than in the original dataset 1 with 4 observations. This can be attributed to the fact that when an observation point is added the value of E calculated in each iteration considers the total error in five wells instead of four. Thus, when an observation well is added an increase in E is to be expected, as is an improved estimate of L and Q.

5.4 Discussion of the Field Application

The application of the AEM and inverse algorithm to the field site illustrated the importance of understanding the characteristics of the site. The flow field resulting from the forward modeling of parameter set one and the initial guess values for L and Q was observed to contain unrealistic head contours at the boundaries. Observation of ***Figure 4.6*** indicated that there was a disconnect between parameter set one and what local values were likely to be. The large value entered for flow in the upper aquifer forced the heads in the upper aquifer to range from 150 ft to 280 ft. It was known that the heads in the area were closer to 215 ft to 220 ft.

The error function associated with the inverse solution to Parameter Set 1 is misleading. The error function itself is relatively low, however the values of the

individual heads have an opposite vertical gradient than those at the site. This can be attributed to the proximity of the well screens in ***Figure 4.6*** to the 210 ft contour. This is indicative of the non-uniqueness associated with the technique and some additional knowledge of system behavior must be used to constrain the inverse model.

For this reason, as well as the head values in the resulting flow field, it was determined that the values in parameter set one were not an accurate representation of the site. The flow field resulting from the initial guess for L and Q and parameter set two contains head values that are much closer to what would be expected at the site, ***Figure 4.7***.

The flow field produced by the average values of L and Q identified by the inverse algorithm, ***Table 4.7***, is very similar to the flow field created by running the AEM with the initial guess values, ***Figure 5.1***. This is due to the fact that the initial guess values for L and Q already produced a very low error function and a reasonable flow field.

It is noted in the comparison between ***Figures 4.6 and 4.7*** that the parameters describing flow and hydraulic conductivity in the lower and upper aquifers have a significant effect on the flow fields predicted by the inverse application of Anderson's AEM. With an understanding of what values are to be expected in the flow field it can be assessed whether or not reasonable values have been chosen for the site.

The values for *window length* and *flow through the window* are only representative of what is occurring at the location of the vertical plane in the window that contains the observation wells. Both parameters are only valid for a unit width into the z-plane. In this study all results in this study are considered over a unit width.

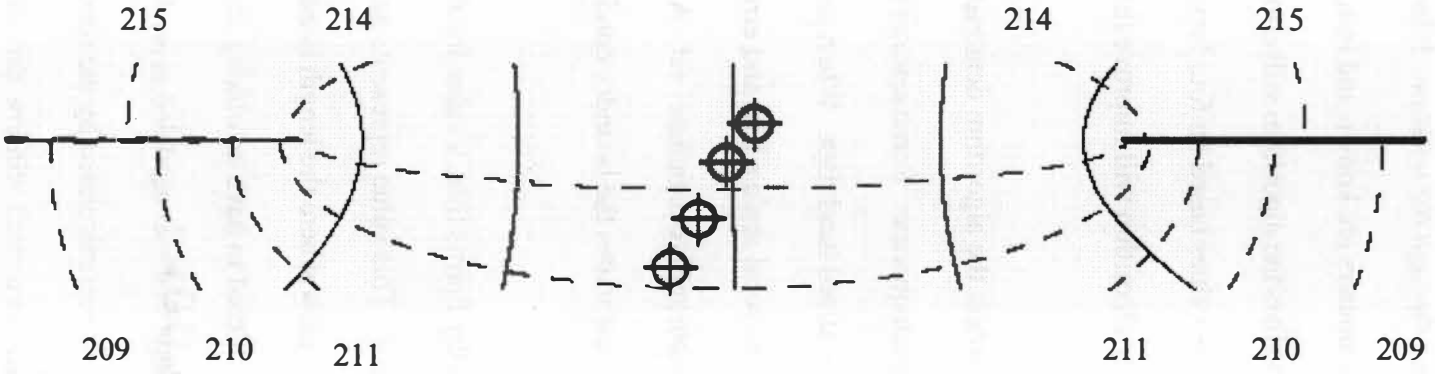

Dataset 7/12/2004

Figure 5.1 Flow Field Map of the Average Inverse Solution at Shelby Farms- Parameter Set One

This figure represents a vertical cross section through a window of unit width normal to the vertical plane. All head values are presented in feet.

L=5250 ft Q=-573.9 ft^3/day

---------- Head Contours

_____ Flow Paths

⊕ Location of Well-Screen Center

500 ft

Scale

6 Conclusions

The analytical element model developed by Anderson (2001) can be solved inversely for the parameters *window length* and *flux through the window*. It has been illustrated that when the exact values of locked parameters are known and initial estiments of L and Q are within 100% of the true values the algorithm will converge onto an estiment of L and Q that is within 20% of the true values based on four head observations. Adding a fifth head observation to the algorithm will improve the accuracy of the estiments of L and Q.

In the case of the Shelby Farms field experiment the algorithm demonstrated a problem, as with most inverse techniques, with nonuniqueness. Some *apriori* knowledge must be used to constrain the search beyond just localized head data. When parameter selections include values that differ on a regional and local scale a trial and error approach can be used in the selection of the most appropriate parameter set. A parameter should be chosen that results in a solution that best estimates the boundry conditions that exist at a site (such as flow gradient).

When the algorithm was applied to the Shelby Farms Site, a value for *flux through the window* was estimated to be -525 ft^3/day. This value represents an estimate of the flow occuring through a unit width of the window where the length is estimated to be 574 ft. Given that the window is generally considered to have an oblong shape (Graham and Parks, 1986) and that the vertical plane that was modeled is on the major axis of the window, these values are comparable to those calculated by the modeling preformed by Gentry et al. (2004) which determined an overall window flux of approximately 35,626 ft^3/day.

Bibliography

Anderson, E.I., 2001, Conformal mapping of groundwater flow fields with internal boundaries, Advances in Water Resources, 25 (2002) 279-291, 32p.

Bradley, M.W., 1991, Groundwater hydrology and the effects of vertical leakage and leachate migration on groundwater quality near the Shelby County landfill, Memphis, Tennessee: USGS Water-Resources Investigations Report 90-4075, 42p.

Darcy,H. 1856. Les Fountaines Publiques de la Ville de Dijon. Delmont, Paris.

Gentry, R.W., J. Anderson, J. Carmichael, D. Larsen, L. McKay, K. Solomon, and N. Thonnard, 2004. A Novel Approach for Understanding the Recharge Mechanisms to the Memphis Aquifer in Shelby County – Tailored Collaboration Project 2700, unpublished, 273p.

Gentry, R.W., 2003, Efficacy of genetic algorithm to investigate small-scale aquitard leakage: Journal of Hydrologic Engineering, July 2003, 9p.

Graham, D.D., and Parks, W.S., 1986, Potential for leakage among principal aquifers in the Memphis area, Tennessee: USGS Water-Resources Investigation Report 85-4295, 46p.

Heitzman, G. 1977. Analytical Modeling of Multi-Layered Groundwater Flow. M.S. Thesis, Dep. of Civil Engineering, University of Minnesota, Minnesota 1977

Kacimov, AR, Obnosov, YuV, Steady water flow around parabolic cavities and through parabolic inclusions in unsaturated and saturated soils. Journal of Hydraulics, 2000; 238:65-77

Larson, D., Gentry, R.W., Ivey, S., Solomon, D.K., and Harris, J., 2003, Groundwater leakage through a confining unit beneath a municipal well field, Memphis. Tennessee, USA Shultz, H. D. and Hadeler, A., Eds., Geochemical Processes in Soil and Groundwater: Wiely-VCH, Berlin, p. 51-64

National Research Council (NRC). 2004. *Groundwater Fluxes Across Interfaces.* National Academy Press: Washington, D.C. 85p.

Obdam, ANM, Veling, EMJ, 1987, Elliptical inhomogeneities in groundwater flow - an analytical description, Journal of Hydraulics, 1987

Parks, W.S., and Mirecki, J.E., 1992, Hydrogeology, ground-water quality and potential for water-supply contamination near the Shelby County landfill in Memphis, Tennessee: U.S. Geological Survey Water-Resources Investigations Report 91-4173, 79p.

Polubarinova-Kochina PY, 1962, Theory of groundwater movement, New Jersey: Princeton University Press

Sidiropoulos, E. , C. Tzimopoulos, and P. Tolikas. 1983. Modeling of discontinuities through dipole distribution. Appl. Math. Modeling, 7, October, pp. 306-310

Strack, O.D.L., 1989, Groundwater Mechanics, Prentice Hall, New Jersey: Prentice-Hall, 732p.

Sun, Ne-Zheng, 1995, Inverse Problems in Groundwater Modeling. *Kluwer* Academic Publishers, the Netherlands, 364p

Yeh, W. W. 1986. Review of Parameter Identification Procedures in Groundwater Hydrology: The Inverse Problem. *Water Resources Research*. 22(2):95-108.

Appendix
FORTRAN Source Codes

```
c
c
c
c            Conformal Mapping Analytical Tool
c
c                  Shelby Farms Site
c
c                   July 14, 2004
c
c                   Patrick Lasater McMahon
c
c ************************************************************************
c
c   *** Explicitly reference variable types ***
c
c
c
c
      Real*4 l,qxu, qxl, q, k, ku, kl, b, phiu, psi(160,1000),x,y,
     & stream(160,1000)
          complex z(160,1000), zeta(160,1000), o(160,1000)
          integer*4 i,j

c   *** Open output and input files  ***
c
c
      open(unit=20,file ='conformal.in',status='old')
          open(unit=40,file='con_head.out',status='new')
          open(unit=50,file='con_stream.out',status='new')
          open(unit=41,file='well_heads.out',status='new')
c
c
c   ***  Read Input data ***
c
      read(20,*) l,qxu, qxl, q, ku, kl, phiu,b
c
c
c   ***  Establish z matrix ***
c
c
c
      pi=3.14159265359
c
      x=-501
          y=-56
```

```
      do 20 i=1, 1000
           do 10 j=1, 55
            z(j,i) = cmplx (x+i,-(y+j))
 10        continue
 20    continue
       x=-501
           y=-56
           do 25 i=1, 1000
            do 23 j = 56, 160
            z(j,i) = cmplx (x+i,-(y+j))
 23      continue
 25    continue



c  ***   Perform calculations  ***
c
      k=(kl-ku)/(kl+ku)
c
c
      do 40 i = 1,1000
           do 30 j = 1,160
            if(aimag(z(j,i)).ge.0.0)then
             zeta(j,i)=-(2./l)*(z(j,i)-sqrt(z(j,i)-l/2.)*sqrt(z(j,i)+l/2.))
            else
             zeta(j,i)=-(2./l)*(z(j,i)+sqrt(z(j,i)-l/2.)*sqrt(z(j,i)+l/2.))
            endif
 30         continue
 40    continue
c
      do 60 i = 1, 1000
           do 50 j = 1, 55
           o(j,i) = qxl*(l/4)*(1-k)*zeta(j,i)+qxu*(l/4)*((1/zeta(j,i))-k*zet
     &a(j,i))+(q/pi)*clog(zeta(j,i))+phiu
           psi(j,i) = real(o(j,i)/(ku*b))
           stream(j,i) = aimag(o(j,i))
 50     continue
 60    continue
c
      do 80 i = 1,1000
           do 70 j=56,160
           o(j,i)=qxl*(l/4)*((zeta(j,i)+(k/zeta(j,i))))+qxu*(l/4)*
     &((1+k)*(1/zeta(j,i)))+(q/pi)*clog(zeta(j,i))+phiu*(kl/ku)
           psi(j,i) = real(o(j,i)/(kl*b))
           stream(j,i) = aimag(o(j,i))
```

```
 70   continue
 80  continue
c  ***   Write well output file   ***

        write(41,300) psi(149,470),psi(116,490),psi(76,510),psi(49,530)
c
c  ***  Write ASCII Grid Import File  ***
c
    write(40,200)
         write(50,200)
         do 100 j=1, 160
          do 90 i = 1, 1000
          write (40, 300) psi(j,i)
          write (50, 300) stream(j,i)
90     continue
100   continue
c
c
200   format('ncols 1000',/,'nrows 160',/,'xllcorner -500',/,
   &'yllcorner -105',/,'cellsize 1')
c
 300  format(f15.5,' ',$)
c
c
        end
```

```
c
c
c
c            Conformal Mapping Analytical Tool
c
c                  June 7, 2004
c
c             Patrick McMahon and Randy Gentry
c
c**********************************************************************
c
c   *** Explicitly reference variable types
c
c
c
c
     Real*4 l,qxu, qxl, q, k, ku, kl, b, phiu, psi(1000,1000),x,y,
    & stream(1000,1000)
         complex z(1000,1000), zeta(1000,1000), o(1000,1000)
         integer*4 i,j
c
c     Real*4 l,qxu, qxl, q, k, ku, kl, b, phiu, psi(1000,1000),x,y,
c    & stream(1000,1000)
c         complex z(1001,1001), zeta(1001,1001), ou(1001, 501), ol(1001,500)
c         integer*4 i,j
c
c
c   *** Open output and input files  ***
c
c
     open(unit=20,file ='conformal.in',status='old')
         open(unit=40,file='con_head.out',status='new')
         open(unit=50,file='con_stream.out',status='new')
         open (unit=60, file='grid.out',status='new')
c
c
c  ***  Read Input data ****
c
     read(20,*) l,qxu, qxl, q, ku, kl, phiu,b
c
c
c  ***  Establish z matrix ***
c
c
c
```

```
      pi=3.14159265359
c
      x=-0.5
           y=-0.500
      do 20 i=1, 1000
           do 10 j=1, 499
            z(j,i) = cmplx (x+i/1000.,y+j/1000.)
 10        continue
 20   continue
      x=-0.5
           y=0.001
           do 25 i=1, 1000
            do 23 j = 500, 1000
             z(j,i) = cmplx (x+i/1000.,y+(j-500)/1000.)
 23     continue
 25   continue
c
c
      write (60, 200)
           do 28 j = 1, 1000
            do 27 i = 1, 1000
             write(60, 300) real(z(j,i))
 27     continue
 28     continue
c
c
c     do 20 i=0, 1000
c          do 10 j=0, 1000
c           z(j+1,i+1) = cmplx (y+j/1000.,x+i/1000.)
c 10       continue
c 20    continue
c
c  ***   Perform calculations  ***
c
      k=(kl-ku)/(kl+ku)
c
c
c     do 40 i = 1,1001
c          do 30 j = 1, 1001
c           zeta(j,i)=(-2./l)*(z(j,i)-csqrt((z(j,i)-(l/2.))*(z(j
c    &,i)+(l/2.))))
c
      do 40 i = 1,1000
           do 30 j = 1, 1000
            if(aimag(z(j,i)).ge.0.0)then
```

```
          zeta(j,i)=-(2./l)*(z(j,i)-sqrt(z(j,i)-l/2.)*sqrt(z(j,i)+l/2.))
         else
          zeta(j,i)=-(2./l)*(z(j,i)+sqrt(z(j,i)-l/2.)*sqrt(z(j,i)+l/2.))
         endif
 30      continue
 40   continue
c
c
c
c     do 60 i = 500, 1001
c         do 50 j = 1, 1001
c         ou(j,i-499.) = (qxl*(1-k)-qxu*k)*(zeta(j,i)*l/4.)+(qxu*l/(4.*
c     &zeta(j,i)))+(q/pi)*clog(zeta(j,i))+phiu
c         psi(j,i) = real(ou(j,i-499.))/ku*b
c         stream(j,i) = aimag(ou(j,i-499.))
c
     do 60 i = 1, 1000
         do 50 j = 500, 1000
         o(j,i) = qxl*(l/4)*(1-k)*zeta(j,i)+qxu*(l/4)*((1/zeta(j,i))-k*zet
    &a(j,i))+(q/pi)*clog(zeta(j,i))+phiu
c         o(j,i) = (qxl*(1-k)-qxu*k)*(zeta(j,i)*l/4.)+(qxu*l/(4.*
c     &zeta(j,i)))+(q/pi)*clog(zeta(j,i))+phiu
         psi(j,i) = real(o(j,i)/(ku*b))
         stream(j,i) = aimag(o(j,i))
 50    continue
 60   continue
c
c
c
c     do 80 i = 1,500
c         do 70 j=1,1001
c         ol(j,i)=(qxl*(l/4.)*zeta(j,i))+(qxl*k+qxu*(1+k))*(l/(4.*zeta(
c     & j,i)))+((q/pi)*clog(zeta(j,i)))+((kl/ku)*phiu)
c         psi(j,i) = real(ol(j,i))/kl*b
c         stream(j,i) = aimag(ol(j,i))
c
     do 80 i = 1,1000
         do 70 j=1,499
         o(j,i)=qxl*(l/4)*((zeta(j,i)+(k/zeta(j,i))))+qxu*(l/4)*
    &((1+k)*(1/zeta(j,i)))+(q/pi)*clog(zeta(j,i))+phiu*(kl/ku)
c         o(j,i)=(qxl*(l/4.)*zeta(j,i))+(qxl*k+qxu*(1+k))*(l/(4.*zeta(
c     & j,i)))+((q/pi)*clog(zeta(j,i)))+((kl/ku)*phiu)
         psi(j,i) = real(o(j,i)/(kl*b))
         stream(j,i) = aimag(o(j,i))
 70    continue
```

```
 80   continue
c
c
c  ***  Write ASCII Grid Import File  ***
c
     write(40,200)
          write(50,200)
          do 100 j=1, 1000
           do 90 i = 1, 1000
           write (40, 300) psi(j,i)
           write (50, 300) stream(j,i)
90     continue
100   continue
c
c
200   format('ncols 1000',/,'nrows 1000',/,'xllcorner -0.5',/,
    &'yllcorner -0.5',/,'cellsize 0.001')
c
 300  format(f15.5,' ',$)
c
c
          end
```

Vita

Patrick McMahon is a Tennessee native born in Chattanooga in 1979 and raised in Knoxville. He graduated from Farragut High School in 1998 and attended the University of Tennessee on a full scholarship. Patrick earned his Bachelor of Science degree in Civil Engineering with a minor in Environmental Engineering in 2003. Currently he is a graduate student at the University of Tennessee pursuing a Master of Science degree in Environmental Engineering.